

Nenwin: an alternative to Neural Networks

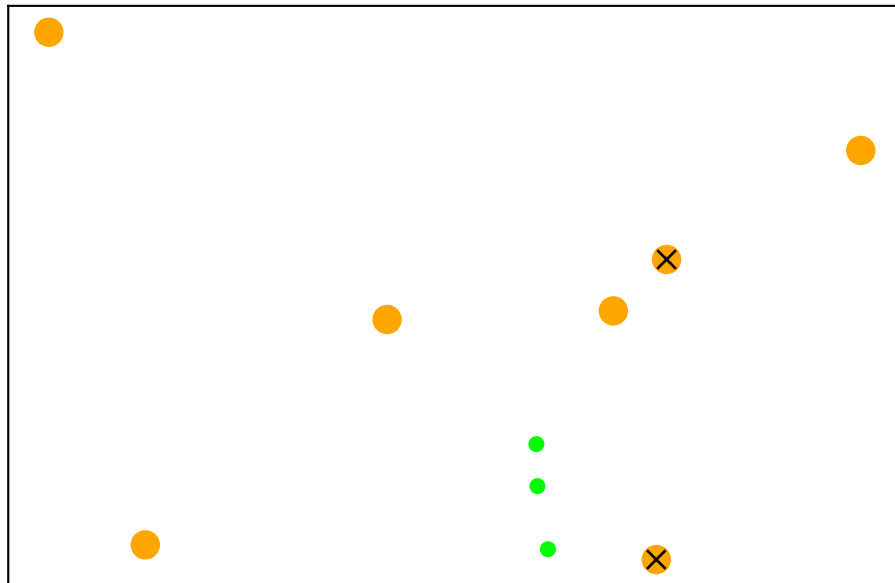
Lulof Pirée

`lulof.piree@zoho.com`

Honors Academy - Eindhoven University of Technology

May 27, 2021

This work describes an alternative modelling framework to neural networks, based on particle simulation. Theory is derived for optimizing models in this framework with backpropagation. An implementation and exploratory empirical results of optimizing a model are presented. Furthermore, it is proven that the framework it is Turing-complete, by showing informally how the new algorithm could emulate a CPU. Finally, proposal are made how the simulation algorithm can be improved in memory and runtime efficiency.



Contents

1	Introduction	4
1.1	Outline	5
2	Algorithm Description	5
2.1	Objects	5
2.2	MarbleEaterNodes	7
2.3	Motivation Emitter Nodes	7
2.4	EmitterNode	8
2.5	Particle attributes	9
2.6	Application to Machine Learning	11
2.6.1	Input Placement	11
2.6.2	Simulation	12
3	Reductions	14
3.1	NAND-gate	15
3.2	Tunnel	23
3.3	Bit register	25
3.3.1	Architecture	25
3.4	Clock and divider	31
3.5	Section conclusion	34
4	Training and backpropagation	35
4.1	EaterNodes as output	35
4.2	Loss definition	36
4.2.1	Classification loss	36
4.2.2	Multiple outputs	38
4.2.3	Non-convexity	38
4.2.4	Loss gradient	41
4.3	Backpropagation of mass-gradient through MarbleEmitterNodes	42
4.4	Backpropagation of pos-, vel- and acc-gradient through MarbleEmitterNodes	43
4.5	Non-propagatable gradients	44
4.6	Backpropagation discussion	44
5	Experimental results	45
5.1	Dataset description	45
5.2	Architectures	46
5.3	Setup	47
5.4	Results	47
5.4.1	Evaluation eccentric run	50
5.4.2	A stable run with good performance	52

6	Complexity	53
6.1	Beeman's Algorithm	53
6.2	Runtime complexity	53
6.3	Backpropagation memory complexity	54
7	Runtime complexity optimization	56
7.1	Limiting to neighbouring particles	56
7.2	Application to Nenwin	57
8	Discussion	63
8.1	Extendability of Nenwin	63
8.2	Practical limitations	63
8.2.1	Unexplored hyperparameters	63
8.2.2	Statistical significance	64
8.3	Loss function	64
8.4	A broader view	64
9	Conclusion	65
10	Acknowledgements	65
	References	65

1 Introduction

Neural networks, such as Multilayer Perceptrons, Recurrent Neural Networks (e.g. the GRU [5]), Convolutional Neural Networks (e.g. the famous AlexNet [11]) and many more, are a popular class of trainable models for Artificial-Intelligence and datamining applications. Neural networks are a series of interconnected functions consisting of an affine map followed by a nonlinear activation function, such as the hyperbolic tangent. In essence, they are a trainable nonlinear functions. One may object that Recurrent Neural Networks are no functions, as they have a state. But they can be seen as a function that takes its own output back as an additional argument: their computation remains the same.

Simulation of physical particles is a well-established technology for scientific research, for example used in astronomy and chemistry. These simulations consist of a model incorporating physical laws, and individual particles that interact according to these laws. This can for example be used to predict the motion of particles. Many textbooks and even more articles are available on this topic, for example [1], [9] and [3].

Humans, however, are not regarded as functions (the behavioural approach of psychology, which studied humans and other animals as functions, has now mostly been deprecated [12]). Their behaviour can change over time. Given the exact same environment at a later moment in time, humans may behave differently than they did the previous time.

This work explores a new machine learning framework based on particle simulation, that is designed to capture this flexibility of behaviour better. It is based on classical Newtonian mechanics, so the interaction between particles can be compared to interactions between stars, planets and asteroids. A set of particles forms a model, and their *initial* positions, *initial* velocities and masses are their learnable parameters. Input data is represented by particles as well, and their movement is governed by gravitational interactions with the particles in the model. The eventual position of the input particles is used to determine the output. Because these input particles can also attract the particles of the model, the model can change its shape, which in turn changes its computations. Hence the algorithm encoded in the model can, in theory, change over time, without retraining.

It should be noted that the new framework, to be called NENWIN from now onward, is designed for applications in which it either needs to act as an active agent, such as robotics or games, or needs to generate different output over time, such as music generation. For tasks such as image classification it does not provide any benefit over Neural Networks, and such tasks are only of interest for verification purposes.

All source code written for this project is available at <https://github.com/Nifrec/nenwin> under the open-source AGPL-3.0 licence[8].

1.1 Outline

This report will begin with a description the NENWIN framework: the different particles involved, their parameters and the simulation algorithm. Also the motivation for including certain particles will be explained.

The second part of this work will elaborate on theoretical capabilities of NENWIN, namely Turing-completeness. It will be proven, relatively informally, that NENWIN is able to simulate a CPU of the RAM model of computation, which is equivalent in computational power to a Turing Machine.

The third section will describe how the backpropagation algorithm can be applied to a NENWIN simulation. It will explain how various parameters are computationally related to the output of a NENWIN model, and a loss function for a classification tasks will be defined.

The fourth section will present the empirical results of an implementation of the backpropagation algorithm. No robust statistical analysis of the impact of hyperparameters on the performance will be given, but instead the behaviour of the training algorithm will be elaborated for a particularly interesting run, in learning curves and an evaluation of the changes made to the model.

The fifth and sixth section will analyse the runtime and memory issues of the implementation, and propose modifications for the algorithm to improve on this. The implementation and empirical evaluation of those modifications were unfortunately beyond the scope of this study.

Finally, the report will finish with a discussion of limitations and directions of future work, and summarize the main points in a conclusion.

2 Algorithm Description

This section will describe the basic design of the NENWIN scheme. Note that NENWIN represents a class of algorithms, similar to neural networks: each network encodes a different algorithm, but the underlying mechanics are the same. Here the underlying mechanics of NENWIN will be explained.

2.1 Objects

NENWIN is best described by defining a family of objects known as particles. The scheme uses a subspace of \mathbb{R}^n , often $n = 2$ is used in this report to support visualizations, but

any higher dimensionality can be used as well. Each particle has a position, a velocity and an acceleration, which are all vectors in \mathbb{R}^n . Each particle has a mass (i.e. a decimal value, *allowed to be negative*) as well, and its acceleration is at any point in governed by Newton's Second Law [14] and a force vector \vec{f} :

$$p.acc = \frac{1}{p.mass} \sum_{\vec{f} \text{ acting on } p} \vec{f} \quad (1)$$

Where $p.acc$ and $p.mass$ are the acceleration and mass of any particle p .

Note that these forces can only be caused by other particles. Each particle has an associated *attraction function*, that describes what force the particle exerts on any other particle. Although many different functions can be used for this purpose, a natural first choice would be the gravity function (with the constant factor G (the gravitational acceleration) replaced by 1):

$$|\vec{f}| = \frac{p_1.mass \cdot p_2.mass}{|p_1.pos - p_2.pos|^2}. \quad (2)$$

The direction of the force is the direction from the first particle to the second particle, so the force vector is given by:

$$\vec{f} = \frac{p_1.pos - p_2.pos}{|p_1.pos - p_2.pos|} \cdot \frac{p_1.mass \cdot p_2.mass}{|p_1.pos - p_2.pos|^2}. \quad (3)$$

Particles are divided into two general subclasses: Nodes and Marbles. Nodes are used to represent an architecture, they are the fixed part of a NENWIN network that encodes an algorithm. Nodes are further subdivided into MarbleEaterNodes and MarbleEmiterNodes, as described later. Marbles represent input and output data, and are created at runtime. Marbles can keep an optional reference to the datum they represent.

Particles *experience* forces exerted on them by other particles, but also *exert forces onto* other particles. Unlike in classical mechanics, NENWIN does not require these forces to be symmetric. To regulate the *experienced* forces, each particle p has the attributes `marble_stiffness` and `node_stiffness`. These act as multipliers for experienced forces, and are required to be real values in $[0, 1]$. The forces that each particle p exerts onto other particles, is regulated in a similar way: p has two attributes `marble_attraction` and `node_attraction`, act as multipliers of the force that p exerts onto other particles. Also these attributes must be real values in $[0, 1]$.

To summarize, the motion of a particle p is described by the following differential equa-

tions:

$$p.pos = p.pos_0 + \nabla p.pos \cdot t = p.pos_0 + p.vel \cdot t \quad (4)$$

$$p.vel = p.vel_0 + \nabla p.vel \cdot t = p.vel_0 + p.acc \cdot t \quad (5)$$

$$\begin{aligned} \vec{f}_{net} = & \text{marble_stiffness} \cdot \sum_{\text{Marbles } m \text{ acting on } p} \frac{p.mass \cdot m.mass}{|p.pos - m.pos|^2} \\ & + \text{node_stiffness} \cdot \sum_{\text{Nodes } n \text{ acting on } p} \frac{p.mass \cdot n.mass}{|p.pos - n.pos|^2} \end{aligned} \quad (6)$$

$$p.acc = \frac{\vec{f}_{net}}{p.mass} \quad (7)$$

Where t denotes the amount of time passed, and $p.pos_0$ and $p.vel_0$ the initial position and velocity respectively of the particle when it was created. The acceleration of p depends the forces p experiences. These forces are a function of p 's relative distances to other Marbles and Nodes (the denominators in (6) are distance measures). These distances depend on the value of $p.pos$ and the motion of other particles. Hence $p.pos$, $p.val$ and $p.acc$ are highly dependent on the other particles in a NENWIN model, and can change significantly even when only an very small amount of time passes.

2.2 MarbleEaterNodes

To enable output production, a subclass of Node called the *EaterNode* (or more specifically, the *MarbleEaterNode*) is defined: each member of this class has a real-valued radius. A Marble will be removed from the simulation as soon as the distance between the Marble and any MarbleEaterNode becomes smaller than the radius of the MarbleEaterNode: it was 'eaten' by the MarbleEaterNode. The MarbleEaterNode keeps both a count of the amount of Marbles consumed, and a set of references to the associated data of the consumed Marbles.

2.3 Motivation Emitter Nodes

NENWIN will have a nonincreasing amount of particles if only Marbles, Nodes and MarbleEaterNode would be used. Marbles can be removed when eaten by a MarbleEaterNode, but the there is no internal way the system can produce new Marbles (other than awaiting new input). This would imply that the amount of information that can be stored in a NENWIN simulation is also nonincreasing in a NENWIN architecture.

Turing Machines, on the other hand, can *increase* the information stored on their tape. For example, consider a Turing machine that writes down all binary numbers, starting with 0. Let this Turing machine be constructed such that it leaves a blank ('□') to the left of this 0, and then writes the next number (1), and leaves another blank and writes

the next number (01), and so on. Then if given a tape of only blanks, it will continue to write an infinite amount of binary numbers on it. For any reasonable definition of information, this would clearly increase the total amount of information on the tape.

2.4 EmitterNode

To make NENWIN able to increase the amount of information, we define an additional particle called the *EmitterNode* (or, more specifically, a *MarbleEmitterNode*¹). EmitterNodes are a subclass of MarbleEaterNodes, but besides eating they can also (conditionally) create new particles at its own position.

There are many different ways to choose the exact behaviour of MarbleEmitterNodes, but in this paper we use the following:

- A MarbleEmitterNode is a special case of a MarbleEaterNode, and tracks also the cumulative mass of Marbles it has consumed in a field `stored_mass`.
- The MarbleEmitterNodes can only create Marbles with predefined parameters (mass, initial velocity, etc.) *near* its own position.
- At a fixed time interval, the MarbleEmitterNode will create a new Marble and subtract its mass from `stored_mass`, unless `stored_mass` is smaller than the mass of the would-be created Marble.
In case the mass of the Marble is negative, it will only be created as long as the `stored_mass` is *at most* the value of the mass of the Marble (i.e. the `stored_mass` is also negative, and has a magnitude at least as great as the magnitude of the mass of the Marble).
- The created Marble must be within the radius or at an infinitesimal distance from the border of the radius of the MarbleEmitterNode. In case the Marble is within the radius it will be consumed immediately, hence only the infinitesimal distance is a practical option. In implementation, where infinitesimal numbers cannot be represented, a small constant $\epsilon > 0$ can be defined such that we require (if *emitter* is the MarbleEmitterNode that creates Marble *m*):

$$emitter.radius < distance(emitter.pos, m.pos) \leq emitter.radius + \epsilon \quad (8)$$

(More informally, MarbleEmitterNodes may only emit Marbles as close to the circumference of their radius as possible, but without immediately eating the Marble again).

To see how EmitterNodes can be used to create any arbitrary amount of entropy, consider an EmitterNode that generates Marbles with infinitesimally small mass, or even 0 mass.

¹Note that there is no theoretical objection against creating EmitterNodes that emit other Nodes, other than the fact that EaterNodes cannot eat each other at the same time.

After eating a Marble with a finite mass, it will be able to generate infinitely many new Marbles. If a dynamic system guides the movement of the Marbles, then each can eventually take on a unique position (since they are not created at the same moment, and the system is dynamic, they will follow a different path). Any information can be encoded in the distribution of these Marbles, which implies that the amount of information in the simulation can be increased in the same way as a Turing Machine can increase the information on its tape.

See 1 for a diagram the complete particle hierarchy.

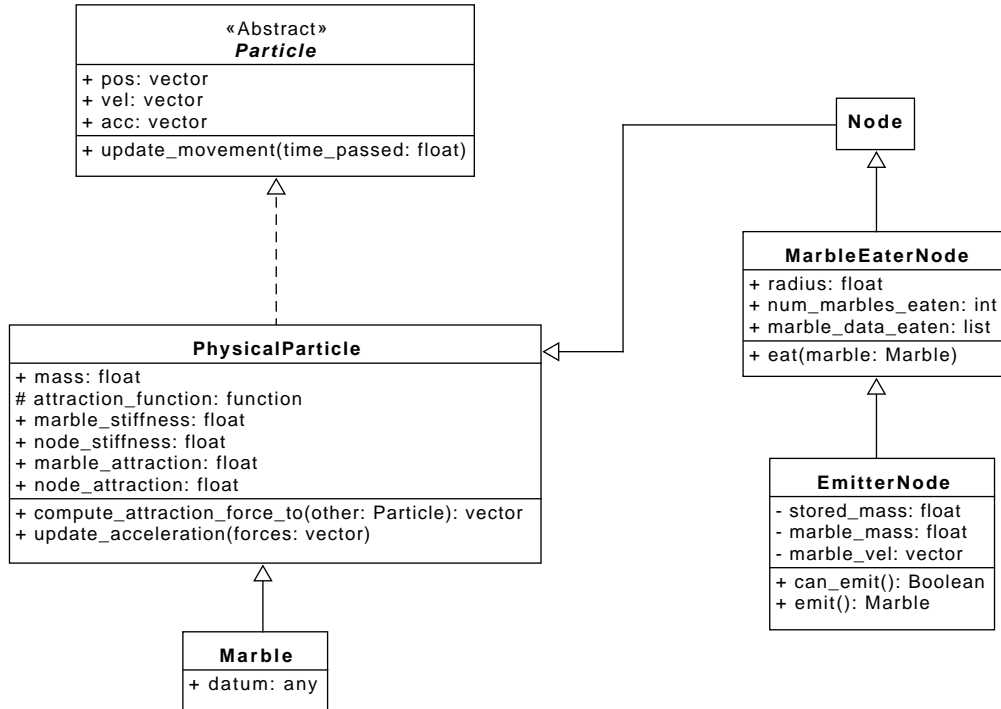


Figure 1: UML class diagram depicting the inheritance relations between different particles. Note that the exact inheritance and attribute-visibilitys may vary between implementations. For example, in the provided implementation, Marble is a subclass of Node.

2.5 Particle attributes

An overview of the different attributes per particle subclass is given in Table 1.

Attribute	type	Marble	Node	MarbleEaterNode	EmitterNode
pos	\mathbb{R}^n	✓	✓	✓	✓
vel	\mathbb{R}^n	✓	✓	✓	✓
acc	\mathbb{R}^n	✓	✓	✓	✓
marble_stiffness	$[0, 1]$	✓	✓	✓	✓
node_stiffness	$[0, 1]$	✓	✓	✓	✓
marble_attraction	$[0, 1]$	✓	✓	✓	✓
node_attraction	$[0, 1]$	✓	✓	✓	✓
attraction_function	$f : \mathcal{P} \times \mathcal{P} \rightarrow \mathbb{R}^n$	✓	✓	✓	✓
datum	any object	✓			
eaten_marbles	stack of Marbles			✓	✓
radius	\mathbb{R}			✓	✓
stored_mass	\mathbb{R}			✓	✓
spawnpos	\mathbb{R}^n				✓
prototype_marble	Marble				✓

Table 1: A summary of different attributes used by different particles. ✓ indicates a particle has the certain attribute. \mathcal{P} is used to denote the set of all particles in a given architecture.

Here **pos**, **vel** and **acc** are the position, velocity and acceleration of a particle, which are real vectors defined in \mathbb{R}^n where n is the dimensionality of the architecture. The stiffness and attraction values are real numbers in the interval $[0, 1]$. The attraction function maps two particles to a vector of the same shape as **acc**.

The **datum** is any data-element that a Marble represents, and this attribute is allowed to be valueless.

eaten_marbles is a stack of all Marbles a MarbleEaterNode (or its subclass, a MarbleEmitterNode) has consumed, with the latest consumed Marble on top of the stack. This stack is allowed to be empty.

The **radius** of a MarbleEaterNode is the maximum distance such that, if a Marble is at this distance or at a smaller distance to the MarbleEaterNode, it will be consumed.

The **stored_mass** is the cumulative mass of the Marbles in **eaten_marbles** of a MarbleEmitterNode, minus the cumulative mass of emitted Marbles. This value is allowed to be negative, which is required to emit negatively-massed Marbles.

The **spawnpos** is the relative position from the center of an MarbleEmitterNode at which a Marble can be created when emitted, this point is at most **radius** + ϵ away from the center of the MarbleEmitterNode, where ϵ is an infinitesimal number. The prototype Marble is a 'blueprint' of the Marble that is emitted: all its attributes are copied to a new Marble that is being emitted, except the position (which is governed by the combination of the position of the MarbleEmitterNode and **spawnpos**), the velocity and the acceleration (which are set to $\vec{0}$).

2.6 Application to Machine Learning

NENWIN is designed to fulfil the role of a decision-making agent, for example as an alternative to neural networks in reinforcement learning or classification tasks. Besides simulating particles, this would also require the system to receive input and produce output.

For example, if a NENWIN simulation is used as an agent to play a game, say chess, then it must be able to perceive the current state of the game, and to choose a move to make. As for another example, if a NENWIN simulation is used for an image classification task, then it must be able to read the images, and output a predicted class.

Adding inputs is straightforward: a region in \mathbb{R}^D (where D is the chosen dimensionality of the NENWIN architecture) is chosen as the *input region* R . If input datapoints are given in \mathbb{R}^n , then one can define a function (an *input placer*) that maps \mathbb{R}^n to a set of Marbles located in R . The inputs can be stored in an bi-directional input/output buffer, called a *channel*. The simulation will then check the channel each timestep, and map any data in the channel to Marbles, and insert these into the simulation.

To produce output, MarbleEaterNodes are used. At each timestep, the simulation outputs a vector containing a natural number for each present MarbleEaterNode into the output of the channel. These natural numbers encode the total number of Marbles eaten by each MarbleEaterNode. This vector can, for example, be interpreted as a one-hot encoding for classification (it contains only one '1' when read as soon as the first Marble has been eaten). For even more detailed output, one can allow external functions to read the exact set of Marbles eaten by each MarbleEaterNode. This latter extension was used for classification training described in a later section.

2.6.1 Input Placement

Marbles are used to represent input data, which can for example be tabular data, an image, a stream of sound or video, etc. From the algorithm's side, this simply means that a new set of Marbles can be added to the simulation at each timestep. However, it is required to map the input data (together with a designated *input region*) to a set of Marbles first, by means of a function called an *input placer*. Such input placers could be defined in many different ways. For example, a datapoint could be used to generate a single Marble, in which the datum is mapped to an attribute of the Marble, such as the position, the mass, the velocity, etc.. It is also possible to use information multiple datapoints to create a single Marble. Furthermore, it is also possible to define a trainable input placer, which can be optimized using machine learning techniques.

It was chosen to use an input placer (the "GridInputPlacer") that simply spreads the Marbles evenly in a two-dimensional grid over the input region (in order of the input

vector, from left to right, top to bottom). This grid-placement generalizes to higher dimensions. The GridInputPlacer creates a Marble for each datapoint at a unique grid-point. Note that this choice is rather arbitrary: as of current there are no arguments why aligning the Marbles in another pattern (such as on a circle) would be less suitable for AI applications.

Two variants of the GridInputPlacer were used:

- MassInputPlacer: maps each datapoint to a Marble, whose mass is set to the value of the datapoint. The initial velocity is by default set to $\vec{0}$. When another velocity vector \vec{v} is used, the notation MassInputPlacer(\vec{v}) will be used.
- VelInputPlacer: maps each datapoint to a Marble, whose velocity is set to a vector of which each element equals the value of the datapoint. It sets the mass of each Marble to 1.0.

All variants set, for each Marble, the remaining attributes as follows:

- the radius of the threshold radius to 100.
- the acceleration to $\vec{0}$.
- the `marble_stiffness` to 1.
- the `node_stiffness` to 0.
- the `marble_attraction` to 0
- the `node_attraction` to 1.

2.6.2 Simulation

See Algorithm 1 below for an abstract pseudocode description how a NENWIN can be simulated. This pseudocode includes input-output handling. Note that in implementation the functionality will be subdivided into different modules. It is for example equally fast, but from an Object-Oriented point of view preferable, to first create Marble instances for new inputs and then sending them over the channel rather than sending the raw data itself. This does not affect the behaviour of the algorithm.

Algorithm 1:

NENWIN(**nodes**, **input_space**, **placement_function**, **mass_function**,
channel, **attraction_function**)

Input: **nodes**: A set of **Node** objects, each having a position, velocity and acceleration in \mathbb{R}^D and a stiffness and a mass in \mathbb{R} .

input_space: A (hyperrectangular) subspace of \mathbb{R}^D . **input_placer**: A function that maps input vectors (in \mathbb{R}^n) to Marbles located in **input_space**.

channel: A bi-directional communication channel over which any finite real-valued vectors can be sent.

attraction_function: A function that maps two Marbles (usually using their masses and their relative distance) to an attraction force vector.

Output: None

```
1 particles ← nodes ;
2 eater_nodes ← [node : node ∈ nodes ∧ node is a MARBLEEATERNODE] ;
   /* The following is a subset of 'eaters': */
3 emitter_nodes ← [node : node ∈ nodes ∧ node is a MARBLEEMITTERNODE] ;
4 while True do
5   if there is input on the channel then
6     for  $\vec{v}$  ∈ channel do
7       | particles ← particles ∪ {input_placer( $\vec{v}$ )};
8   if there is an output request on the channel then
9     output ← a new empty list ;
10    for node ∈ eater_nodes do
11      | output.append(|node.eaten_marbles|) ;
12    Place output on the channel ;
13  for p ∈ particles do
14     $\vec{f} \leftarrow \sum_{o \in \text{particles} \setminus \{p\}} \frac{o.pos - p.pos}{||o.pos - p.pos||} \cdot \text{attraction\_function}(p, o)$  ;
    /* Newton's Second Law */
15    p.acc ← p.mass ·  $\vec{f}$  ;
16  for e ∈ emitter_nodes do
17    if |e.stored_mass| ≥ |e.prototype_marble.mass| ∧ sgn(e.stored_mass) =
      sgn(e.prototype_marble.mass) then
18      | particles ← particles ∪
        {a copy of e.prototype_marble at position e.pos + e.spawnpos}
19  for particle ∈ particles do
20    Compute and update particle's next position and velocity given their
    current acceleration (using numerical integration). ;
21  for marble ∈ particles \ nodes do
22    for node ∈ eater_nodes do
23      if distance(marble.pos, node.pos) ≤ node.radius then
24      | particles ← particles \ {marble} ;
25      | node.stored_mass ← node.stored_mass + marble.mass ;
26      | node.eaten_marbles ← node.eaten_marble ∪ {marble};
```

3 Reductions

NENWIN is able to simulate other computational mechanisms². In particular, this section will demonstrate that NENWIN is able to simulate all required components to implement a CPU. A CPU is an implementation of the RAM-model, which is equivalent to a Turing machine [6].

This section will demonstrate that NENWIN is able to simulate the following components, when using Marbles as data-carrying signals:

- A Boolean NAND-gate with interfaces that use Marbles to transmit and receive information. Note that all binary logical functions such as OR, AND, NOT, NOR, etc. can be implemented from compositions of NAND-gates.
- A single-bit register that can store a state 0 or 1. Note that an arbitrary large composition of bit registers can store an arbitrary large amount of data.
- A clock that creates periodically a signal.
- A *divider*: a component that upon intercepting one Marble, creates multiple Marbles with velocities in different directions. In the context of wires and electricity such devices are not needed, but in the context of discrete Marbles it is required.

These reductions demonstrate that NENWIN is theoretically powerful enough to solve the same problems as the simulated components. However, they are not necessary of any practical use otherwise, as it is slower than directly implementing/simulating the other computational mechanisms they simulate. These reductions use very artificial hand-made (in contrast to automatically optimized) architectures that do not exploit the dynamic nature of NENWIN. This generally allows simpler proofs. For example, immovable Nodes result in much less complex proofs than with moving Nodes.

NENWIN is by default non-terminating, but it can simulate terminating algorithms when a consistent rule is used to determine the moment when output is read. One natural such rule is to read output when all Marble's have disappeared, as the output will not change any more after this point.

Consider a variant of Newton's gravity function, called the 'threshold gravity', that rounds the force to 0 when the radius is sufficiently large:

$$threshold_gravity(p_1, p_2, \theta) = \begin{cases} \vec{0} & \text{if } ||p_1.pos - p_2.pos|| > \theta \\ \frac{p_1.m \cdot p_2.m}{||p_1.pos - p_2.pos||^2} & \text{otherwise} \end{cases} \quad (9)$$

²or, equivalently, other computational mechanisms can be reduced to NENWIN. 'Reduction' causes less ambiguity than 'simulate', as NENWIN is implemented via an simulation itself.

Unless stated otherwise, this threshold-gravity force function (9) will be used as attraction function by all particles in this section.

All figures will use the same convention of drawing particles. A legend of this convention is shown below in Fig. 2.

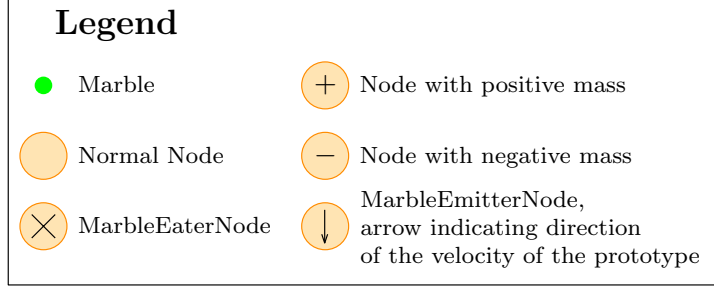


Figure 2: Legend of the figures describing NENWIN architectures. Marbles are depicted as green dots, and nodes as orange disks. MarbleEaterNodes and MarbleEmitterNodes have a special annotation, namely an 'x' for MarbleEaterNodes, and an arrow for MarbleEmitterNodes. This arrow indicates the direction of initial the velocity of emitted Marbles (or, equivalently, the direction of the velocity of the prototype Marble). When relevant for the context, normal Nodes may also be annotated with the polarity of their mass.

3.1 NAND-gate

The NENWIN-scheme is able to simulate a logical NAND-gate. As a NAND-gate is a Boolean function with only two Boolean input values, there are only 4 different input combinations that need to be handled correctly. Below it is shown how NENWIN can directly simulate a NAND-gate with inputs and output to the NENWIN program itself, and how a NAND-gate can be embedded in a larger circuit within a NENWIN-architecture.

Let \mathcal{M} denote the set of all possible marbles and \mathcal{N} the set of all possible nodes.

Lemma 1 (NAND-gate). *There exists an input placer mapping a vector of two Boolean variables to a set of Marbles $f : \{0, 1\}^2 \rightarrow \mathcal{M}^2$, a NENWIN architecture of only nodes $A \subseteq \mathcal{N}$, and a function to map the NENWIN output to a Boolean output $g : \mathbb{N}^2 \rightarrow \{FALSE, TRUE\}$, such that for two Boolean variables $b_1, b_2 \in \{FALSE, TRUE\}$, $g(\vec{y}) = \neg(b_1 \wedge b_2)$, where \vec{y} is the output harvested from architecture A with input $\{f(b_1), f(b_2)\}$ after all marbles were removed from the network.*

Proof. For all particles we will use `node_stiffness` = 0, `marble_stiffness` = 1, `node_attraction`=0 and `marble_attraction`=1.

Define

$$f(b) = \begin{cases} \text{Marble}(pos = [10, 0], vel = \vec{0}, acc = \vec{0}, mass = +10, datum = \text{TRUE}) & \text{if } b = \text{TRUE} \\ \text{Marble}(pos = [10, 0], vel = \vec{0}, acc = \vec{0}, mass = -10, datum = \text{FALSE}) & \text{if } b = \text{FALSE} \end{cases} \quad (10)$$

Let

$$A = [\begin{array}{l} \text{MarbleEaterNode}(pos = [0, 0], vel = \vec{0}, acc = \vec{0}, mass = +10, radius = 5) \\ \text{MarbleEaterNode}(pos = [20, 0], vel = \vec{0}, acc = \vec{0}, mass = -10, radius = 5) \end{array}] \quad (11)$$

Define

$$g(\vec{y}) = \begin{cases} \text{FALSE} & \text{if } y[0] = 2 \\ \text{TRUE} & \text{if } y[0] \in \{0, 1\} \end{cases} \quad (12)$$

Note that the Marbles are placed in the middle of the line-segment between the two Nodes, and that positive masses attract positive masses and repel negative masses, and vice versa. Hence each of the two Marbles will be accelerated in a straight line to the Node with the same polarity of mass as itself, and will be eaten by it.

Now if the input is (TRUE, TRUE), both Marbles will have a positive mass of 10, and both will be attracted to the left Node (at $pos[0] = 0$ with mass +10). This way both will be absorbed by the first Node, and the output will read $g(\begin{bmatrix} 2 \\ 0 \end{bmatrix}) = \text{FALSE}$ as expected.

If the input equals (TRUE, FALSE), (FALSE, TRUE), (FALSE, FALSE), then at least one Marble will be attracted and eaten by the right node (at $pos[0] = 20$ with mass -10), and since there are only 2 Marbles, no more than one Marble will be eaten by the left Node, and the output is $g(\begin{bmatrix} 1 \\ 1 \end{bmatrix})$ or $g(\begin{bmatrix} 0 \\ 2 \end{bmatrix})$, either of which will evaluate to TRUE as expected. \square

See Fig. 3 for a visualization of the proof.

The above lemma does not show how a NAND-gate can be implemented as part of a larger circuit. To construct a NAND gate that can be used as a submodule, it is required that the NAND-gate only attracts particles within a finite region of the real space (in case three dimensions are used, this region will be a strict subset of \mathbb{R}^3). This is needed to ensure that the rest of the circuit can be implemented safely outside this region. Furthermore, the NAND gate needs to have interfaces to the other parts of the circuit at the boundary of this region.

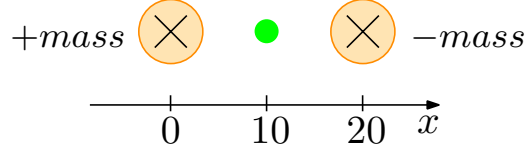


Figure 3: Construction of a NAND-gate in NENWIN as used by the proof of Lemma 1. The left Node has a positive mass, and the right Node a negative mass. Note that only one dimension (the x -axis) is used, and that both Marbles are placed by the input placer on exactly the same position (at $x = 10$).

In the following lemma, such interfaces are represented by MarbleEmitterNodes. The main advantage of user MarbleEmitterNodes is that it gives more control over how the input signal is sent into a circuit module (especially in terms of velocity direction), in comparison to allowing external Marbles to directly enter the module.

The next lemma will show that is possible to extend the NAND-gate with interfaces to an external circuit. It uses the following encodings for TRUE and FALSE: the presence and absence respectively of Marbles with a positive mass (of value α). Note that the direction and velocity of the Marbles emitted by the output MarbleEmitterNodes can be configured. Furthermore, the NAND-gate requires external 'power' to operate: this can be compared to electronic NAND-gates requiring an operating voltage that is separate from the signal. This 'power' needs to be the same for each input, and hence does not externally provide information about the input.

Lemma 2. *Given positive constants $\alpha \in \mathbb{R}$, a finite cuboid $C \subseteq \mathbb{R}^3$, a finite set of particles in a plane $P \subset C$, and an external Marble m_{power} with a mass of $-\alpha$, NENWIN is able to simulate a NAND-gate using two MarbleEmitterNodes at the boundaries of C as interfaces, such that the particles in C influences no particles beyond C except for creating output Marbles. Here TRUE and FALSE are encoded as presence and absence, respectively, of a Marbles with a mass of $+\alpha$. This NAND-gate creates an output after a finite amount of time, and at this time the NAND-gate returns to a state in which it will produce the same output for the same input.*

Proof. The lemma will be proven using a construction. This construction is the concatenation of an AND-gate and a NOT-gate.

Define the following particles in the 'AND' part (also see Fig. 4). All EmitterNodes and EaterNodes will be initialized with a `stored_mass` of 0 and no attraction (which is achieved by setting their `marble_attraction` and `node_attraction` values to 0³):

- A signal-emitter: a MarbleEmitterNode in P with a position and radius such that

³Alternatively, the state of no attraction could be achieved by giving the Nodes a mass of 0. This distinction is not relevant for the proof.

the border of the radius intersects the border of C in one point p . This Node functions as the input interface of the NAND-gate, as zero up to two external Marbles serving as input can be consumed by the signal-emitter at point p . It has a positive emitting-delay of $\delta \in \mathbb{R}$.

- A signal-Marble: the Marble that can be emitted by the signal-emitter. It has of mass α with a positive velocity in the direction of the vector from the signal-emitter towards the center of P (this direction will for convenience be called e_y from now, using the axes as in Fig. 2 we have $up = \begin{bmatrix} x \\ y \\ z \end{bmatrix} = \begin{bmatrix} 0 \\ 1 \\ 0 \end{bmatrix}$). The velocity has a magnitude of v . It has a Marble-stiffness of 0 and a Marble-attraction of 1.
- A signal-accumulator: a MarbleEmitterNode in P placed a distance $d_{AND} \in \mathbb{R}^+$ from the signal-emitter in the direction e_y . d_{AND} is chosen such that the point that is positioned at a positive d_{NOT} in the direction e_y from the signal-accumulator is in C . This Node acts as the logic in the AND-part: it emits Marbles with a mass of 2α , hence it can only emit if the signal-emitter has emitted two Marbles, which only occurs if the signal-emitter has two inputs of value TRUE.
- A resetter-emitter: a MarbleEmitterNode positioned in P , such that it is a distance of $\frac{1}{2}d_{AND} + \psi$ (for a small constant $\psi > 0$) from the center k of the line-segment between the signal-emitter and the signal-accumulator, at an angle in $(0 \text{ deg}, 90 \text{ deg})$ with the line-segment between the signal-accumulator and k . It has a radius such that the border of the radius intersects the border of C . Note that the signal-accumulator, the signal-emitter and the resetter-emitter are all a distance $\frac{1}{2}d_{AND}$ from k . It has an emitting-delay of 2δ .
- A resetter-Marble that can be emitted by the resetter-emitter, which has a mass of $-\alpha$, a velocity of magnitude v and a velocity-direction towards k from the point where it is emitted. It has a Marble-stiffness of 0 and a Marble-attraction of 1. Since it is directed towards k with the same magnitude of velocity as the signal-Marble, these two Marbles will arrive at k after the same time.
- An inhibitor-Marble that can be emitted by the signal-accumulator, and that has a velocity with a magnitude v in the direction e_y .
- Let h be the point in P that is a distance of $\frac{1}{2}d_{NOT}$ away from the signal-accumulator in the direction e_y . It has a Marble-stiffness of 0 and a Marble-attraction of 1.
- A not-emitter: a MarbleEmitterNode placed in P , with a delay of $2\delta + d_{AND} \cdot v$, emitting a Marble (the 'output-Marble') with a mass of α with a velocity with magnitude v in the direction from the not-emitter towards h . The not-emitter is positioned such that the line segment between the not-emitter and h has a length

of $\frac{1}{2}d_{NOT} + \varepsilon$ (for a small constant $\varepsilon > 0$) and does not intersect any Node nor any line segment between a Node and k or h (see Fig. 2). Furthermore, the radius and the position are such that the border of the not-emitter intersects C .

- An output-Marble, as described above, with a Marble-stiffness of 0 and a Marble-attraction of 1.
- An output-emitter: a MarbleEmitterNode that acts as the output-interface. It is positioned in P such that the line between the output-emitter and the not-emitter intersects h , but not any other line segment between a Node and k or h , and such that the border of its radius intersects C .
- An accumulator-resetter-1, a MarbleEmitterNode positioned in P such that if the resetter-Marble is repelled by the signal-emitter, its diverted path will lead to the signal-resetter-1. It has a nonnegative delay β .
- An accumulator-resetter-Marble, that has a positive velocity u in the direction towards a point i on the line segment between h and the signal-accumulator. It has a mass of $-\alpha$, a Marble-stiffness of 0 and a Marble-attraction of 0.
- An accumulator-resetter-2, also a MarbleEmitterNode positioned in P , on the ray that originates from the accumulator-resetter-1 and intersects j , at a greater distance from the first accumulator than j has. It emits an identical Marble as the accumulator-resetter-Marble, but with a velocity directed towards the signal=accumulator. It has a nonnegative delay γ .
- Four garbage-collectors, MarbleEaterNodes all placed in P , that only serve to remove unneeded Marbles. One is placed at a distance d_{NOT} in the direction e_y from the signal-accumulator. Another one is placed at a location where the output-Marble will be recoiled towards (when it arrives at h and the inhibitor Marble is at h plus a distance ε in direction e_y). The third one is placed on the ray that originates in the resetter-emitter and intersects k , at a greater distance from the resetter-emitter than k . The last garbage-collector is placed at a location where the accumulator-resetter-Marble will be recoiled towards from the point j , if it arrives at j while the signal-Marble is a distance ψ from j in the direction e_y .

The resetter-emitter and the not-emitter are the part of the gate that requires 'power', i.e. the NAND-gate only functions if these two MarbleEmitterNodes consume Marbles with an equal mass as the Marble they emit respectively, at the same moment as the input is consumed by the signal-emitter. Note that this 'power' can be supplied without disturbing the interior of C , as these MarbleEmitterNodes intersect the border of C , and the powering Marbles can have a Marble- and Node-attraction of 0.

We now require that, if at some point in time t_0 (w.l.o.g. let $t_0 = 0$) the signal-emitter consumes 0, 1 or 2 Marbles with a mass of α (the presence of a Marble encodes the

input value TRUE, the absence the input value FALSE), and the resetter-emitter and the not-emitter their required powering Marbles, then the NAND-gate should output a Marble with mass α outside of C at a finite point in time $t_{end} > t_0$, unless two input Marbles are provided. We proceed by a case distinction on the number of input Marbles.

1. **0 input Marbles:** this corresponds to the input (FALSE, FALSE). In this case the signal-emitter will not emit any Marble. The resetter-emitter does emit a resetter-marble after a delay of 2δ , as it consumes a powering Marble with a mass of $-\alpha$ at the moment t_0 at which the empty input is 'given'. However, by construction of the NAND-gate, there is no particle or attraction force on the path of the resetter-Marble except for the garbage-collector, which will consume it. Similarly, the not-emitter will be powered and emit a Marble in the direction of the output-emitter, which will also arrive with its original velocity and direction unaffected at the output-emitter. Hence the `stored_mass` of the output-emitter will reach the threshold to emit a Marble with mass α outside of C , which encodes the expected output TRUE.
2. **1 input Marble:** this corresponds to the input (TRUE, FALSE), or to the equivalent case (FALSE, TRUE). Hence the signal-emitter will emit a signal-Marble with a velocity in the direction of e_y . The signal-Marble's velocity will not be affected by the resetter-Marble, since the signal-marble has a Marble-stiffness of 1. There are no other attraction forces or particles along the line segment between the signal-emitter and the signal-accumulator, so the signal-Marble will be consumed by the signal-accumulator. This causes the signal-accumulator to obtain a `stored_mass` of α , which is not sufficient for it to emit a Marble.

The resetter-emitter will also emit a resetter-Marble, which will arrive at the point k when the signal-Marble is a distance ψ in the direction e_y from k (this is, because both Marbles are emitted at the same time in a straight line to k with the same velocity k , only the resetter-emitter needs to travel an additional distance ψ). If the attraction threshold distance of the signal-Marble and the value of ψ have been chosen correctly, then the resetter-Marble will be recoiled by the signal-Marble in a direction different than its original direction (as the signal-Marble is positioned in the direction of e_y from the resetter-Marble, and the repelling force accelerated the resetter-Marble in the direction of the line from the signal-Marble to the resetter-Marble). So by construction the resetter-Marble will be redirected towards the accumulator-resetter-1 (the green arrow in Fig. 4, which in turn will emit a Marble towards the accumulator-resetter-2, which in turn will emit a Marble towards the signal-accumulator. Since this Marble has an opposite mass as the signal-Marble that the signal-accumulator consumed, its `stored_mass` will be reset to 0. It is possible that the negatively-massed Marble will be consumed before the signal-Marble instead, but clearly this leads to the same result ⁴.

⁴Alternatively, γ (the delay of the accumulator-resetter-2) can be adjusted to ensure the signal-Marble will be consumed by the signal-accumulator first. This does not affect the resulting state of the

The rest of the NAND-gate behaves identical as the case of *0 input Marbles*, which leads to the correct output at the output-emitter.

3. **2 input Marbles:** this corresponds to the input (TRUE, TRUE). In this case two signal-Marbles will be emitted, at $t = t_0 + \delta$ and at $t = t_0 + 2\delta$. As in the case of *1 input Marble*, the first signal-Marble will be consumed by the signal-accumulator, and the resetter-Marble will be consumed by the accumulator-resetter-1. Now there exists a value for β (the delay of the accumulator-resetter-1) such that there exists a small constant $\omega > 0$ such that the second signal-Marble is a distance ω in the direction e_y from j when the accumulator-resetter-Marble arrives at j . Similarly to the redirection of the resetter-Marble, this causes the accumulator-resetter-Marble to be redirected, which by construction sends the accumulator-resetter-Marble towards a garbage-collector (the yellow line in Fig. 4).

Hence the signal-accumulator will consume two Marbles each with a mass of α at $t = t_1 = t_0 + 2\delta + d_{AND} \cdot v$ (where $d_{AND} \cdot v$ is the time needed for the second signal-Marble to travel from the signal-emitter to the signal-accumulator), but the accumulator-resetter-emitter-2 will not emit a Marble with negative mass, hence at t_1 the signal-accumulator will emit an inhibitor-Marble. This is also the time at which the not-emitter emits an output-Marble.

Similar to the first signal-Marble, the resetter-Marble and the point k , the output-Marble will arrive at the point h when the inhibitor-Marble is a distance ε in the direction e_y from h . The inhibitor-Marble has a Marble-stiffness of 1, but the output-Marble has a Marble-stiffness of 0 and hence there exists a threshold distance for the inhibitor-Marble and a value for ε such that the output-Marble will be shortly accelerated in the direction of the inhibitor-Marble. Then by construction, the output-Marble will be redirected to an garbage-collector (the purple line in Fig. 4 instead of the output-emitter. Also by construction, the inhibitor-Marble travels in a straight line from the signal-accumulator to a garbage-collector. Hence both particles will be consumed by garbage-collectors. Note that also the signal-accumulator now has a `stored_mass` of 0, as the previously stored mass of 2α has been depleted when emitting the inhibitor-Marble.

It can be concluded that, after the amount of time passed in which the NAND-gate produced output in the *0 input Marbles* and *1 input Marble* cases (which is the same time-span for both cases), no output will be produced, as required by the definition of a NAND-gate.

Note that in all three cases, the NAND-gate eventually returned to the same state as before the input was given, except for the amount of Marbles eaten by the garbage-collectors. But the latter does not affect the behaviour of the NAND-gate, hence it will respond with the same outputs again given any of the three input cases above. \square

particles of the NAND-gate.

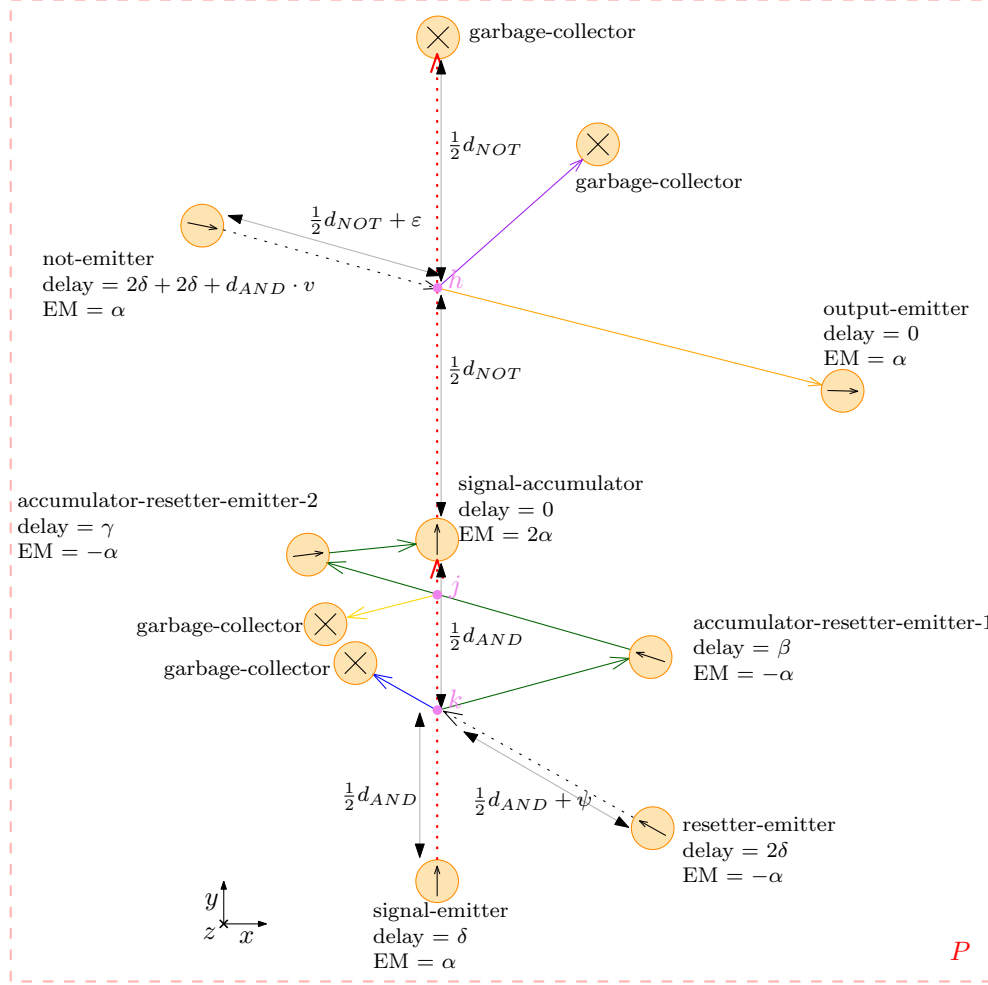


Figure 4: Construction of a NAND-gate in NENWIN as used by the proof of Lemma 2. The axes of spatial coordinates x and y are parallel to the place P . For each MarbleEmitterNode, the emit-delay and the mass of the emitted marble (EM, 'Emitted Mass', for short) have been denoted. MarbleEmitterNodes are marked with an arrow that indicates the direction of the velocity of the Marble they can emit, and the MarbleEaterNodes (that is not also an EmitterNode) has been marked with a cross. Note that the distances between particles and the radii of the Nodes are not to scale.

3.2 Tunnel

Using the the threshold-gravity attraction function (9), is it possible to construct an architecture within a rectangular region that can 'steer' a Marble to any other side of the rectangle, and such that it does not interfere with the architecture outside the rectangle. This is proven in the lemma below. The result can be used as a black box in other proofs to 'tunnel' Marbles from one location to another.

Lemma 3 (Tunnel). *Let $R = [x_0, x_1] \times [y_0, y_1]$ be a rectangle in \mathbb{R}^2 . Let R be free of attraction forces from Nodes and Marbles not in R . Let m be a Marble with nonzero mass that enters (not only intersects) R via an edge l . Then for any point $p = (x_e, y_e)$ on the edges of R that are not l , there exist finite numbers $\epsilon, \theta \in \mathbb{R}$ and a finite set of Nodes such that when placed in R , m leaves R via p .*

Proof. Without loss of generality, assume that l is parallel to the x axis, so all points on l have x coordinates in $[x_0, x_1]$, and the same y coordinate y_l . Let $q = (x_q, y_l) \in l$ be the point where m enters R .

Let h be the line segment between q and the point k , where k is the point where m would have left R if there were no other particles in R . Clearly m would move through R in a straight line segment if R were free of other particles, as R is free of forces from particles outside R , and hence m would have 0 acceleration. Hence k exists.

If $x_0 < x_q < x_1$, then it is possible to place a Node n with threshold gravity at threshold $\theta + \epsilon$, $\theta, \epsilon > 0$ at $(x_n + \theta, y_n) \in R$ such that the entire attraction field of n is in R , $(x_n, y_n) \in h$, $(x_n, y_n) \neq q$ and $0 < \theta \in \mathbb{R}$. If we set $n.mass \leftarrow 0$, then m will leave R at h .

If we make the magnitude of $n.mass$ greater, and set $\text{sgn}(n.mass) \leftarrow \text{sgn}(m.mass)$, and hence the Node's attraction will change m 's course more towards the positive x direction; by correct adjustment of θ and $n.mass$ can clearly adjust the strength of the acceleration and the duration, and hence can steer m to leave R at any point (x_e, y_e) with $x_e > x$ on one of the non- l edges of R .

In a similar way, if we set $\text{sgn}(n.mass) \leftarrow -1 \cdot \text{sgn}(m.mass)$ and place n at $(x_n - \theta, y_n) \in R$ instead, then we can steer m to end up any point (x_e, y_e) with $x_e < x$ on one of the non- l edges of R .

If $x_q = x_0$ or $x_q = x_1$, we can use the requirement that m enters R , which implies that:

1. If $x_q = x_0$, then the x -component of $m.vel$ must be positive, otherwise m 's path would only intersect R (move parallel to an edge or only pass the point q no other point of R), but not enter it.

2. If $x_q = x_1$, then the x -component of $m.vel$ must negative positive, by a similar argument.

In both cases k and h will be well defined, and the construction as of the case $x_0 < x_q < x_1$ can be used. \square

See 5 for a visualization of the construction of the proof.

A conceptually much simpler, but less efficient, method of implementing a 'tunnel' would be to use MarbleEmitterNodes and Marbles, both with 0 Node-attraction and Marble-attraction, in a region of the simulation where no external forces apply: here the Marbles can travel in straight lines between the MarbleEmitterNodes, which provides a method of controlling the movement of Marbles in a sufficiently simple way that it can be designed by hand. One major advantage of this method is that delays can be added to the MarbleEmitterNodes: this way it can be precisely regulated when a Marble will reach the end of the 'tunnel'. Also the velocity magnitude and direction of the resulting Marble emitted by the last MarbleEmitterNode can easily be adjusted.

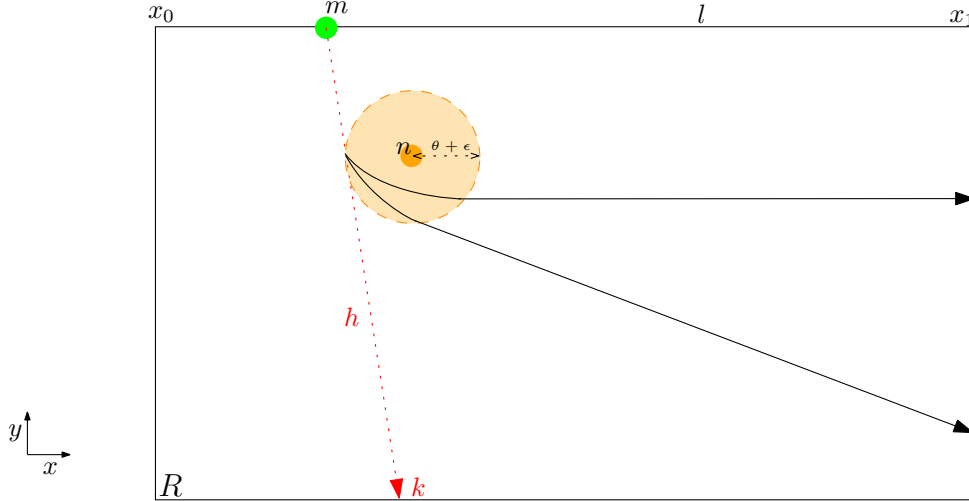


Figure 5: Construction as used in the proof of Lemma 3. The horizontal top edge represents l , bounded by x -positions x_0 and x_1 . m is the Marble, depicted at the position where it intersects the rectangle R first. The red line represents the path of m if there would be no Node in R . The orange point is the node n , and the radius of its threshold function has been drawn in transparent orange. Note that n is θ -distance away from h , horizontally, hence the radius of the attraction will overlap a little with h , which ensures that the movement of m can be influenced by n . The black lines represent possible paths through R of m for two different mass-values of n .

3.3 Bit register

NENWIN can simulate a single-bit register (i.e. an off-on memory cell). We present an architecture, for which we can prove the following properties:

1. It is possible to read the 0 state
2. It is possible to read the 1 state
3. It is possible to set the bit to 0
4. It is possible to set the bit to 1

The register will be operated by sending a Marble to one of 3 (there is one for reading, one for writing and one for erasing the bit) `MarbleEmitterNodes` at the edge of the bit. The output will result in a Marble occurring at one of two specific locations that depend on the bit state. This Marble could from there be redirected, or be consumed by a `MarbleEaterNode`. In the provided architecture the '0-reader' and the '1-reader' are `MarbleEaterNodes` used at these locations, but for different purposes different elements could be placed here.

3.3.1 Architecture

We define the bit architecture \mathcal{B} , implemented in \mathbb{R}^3 as follows:

- Let P be a two-dimensional hyperplane in \mathbb{R}^3 .
- At a specific position in P , we create the center of the bit (the 'bit-position'): in the '1' state, this position is occupied by a specific 'bit-Marble', but empty in the '0' state.
- A 'bit-emitter' `MarbleEmitterNode` is placed along the line l , which runs through the bit position orthogonal to P . We give this `MarbleEmitterNode` a radius such that the edge of the radius is an infinitesimal distance from the bit position. The Marble that it can emit is the bit-Marble at the bit position.
- A 'signal-emitter' `MarbleEmitterNode`, that is placed at a distance from the bit position in P , with a radius sufficiently small not to contain the bit position. The threshold distance is also smaller than the distance from this signal-emitter to the bit-position.
- A 'signal-Marble' that can be emitted by the signal-emitter. This Marble has a positive velocity in the direction from the signal-emitter toward the bit-emitter, and is used to pass an external 'write'-signal received by the signal-emitter to the

bit-emitter. It has the same mass as the bit-Marble.

- Let $\varepsilon \in \mathbb{R}$ be a small yet finite positive number.
- A 'read-emitter' MarbleEmitterNode, that is like the signal-emitter also placed in P with a radius and a threshold sufficiently small not to interfere with the bit position. However, it is placed on a different position than the signal-emitter.
- A '0-reader' MarbleEaterNode that is placed in P on the opposite side of the bit position as the read-emitter, but such that the line between the 0-reader and the read-emitter is a distance ε from the bit position. The radius of this Node can be small but nonzero, and the threshold distance of its attraction is set to 0.
- A 'read-Marble' that can be emitted by the read-emitter, that has an opposite side as the bit-Marble (and hence is repelled by the bit), and a Marble-stiffness of 0. It has a velocity vector in the direction from the read-emitter towards the 0-reader.
- A '1-reader' MarbleEaterNode, that is placed in P at an equal distance from the bit-position as the '0-reader', but located such that it will catch the read-Marble if it is repelled by the bit-Marble: it will be proven below that this is not the same location as that of the 0-reader. The radius and the threshold distance have the same values as in the 0-reader.
- An 'eraser-emitter' MarbleEmitterNode, similar to the signal-emitter, but at a different position.
- A 'garbage-collector' MarbleEaterNode with similar properties as the 0-reader and the 1-reader, but located exactly on the line running from the eraser-emitter to the bit-position, on the opposite side of the bit-position as the eraser-emitter (this is also in P). This Node solely functions to delete Marbles.
- An 'eraser-Marble' that can be emitted from the eraser-emitter, with a velocity in the direction from the eraser-emitter towards the bit-position (and hence also towards the garbage-collector). The mass of this eraser-Marble will have the opposite sign as the bit-Marble, and it will have a Node- and Marble-stiffness of 1. The gravity threshold distance of this eraser-Marble is nonzero.

The Nodes defined above can all be placed in \mathbb{R}^3 , on different positions while satisfying their description. All Nodes and Marbles defined above, except the bit-emitter, are placed in P ⁵.

Note that \mathcal{B} should be placed in a region of \mathbb{R}^3 where no external forces (except for the Marble that activates reading/writing/erasing) apply, and that when using the threshold

⁵It is also possible to place the bit-emitter in P , but this would lead to more complex proofs as we need to ensure that it will not interfere with any Marble moving through P .

gravity function 9.

The particles of \mathcal{B} and their important properties have been summarized in Table 2.

Particle	Type	Mass sign	Marble-stiffness	Marble-attraction
bit-Marble	Marble	-	0	1
bit-emitter	MarbleEmitterNode	0		
signal-emitter	MarbleEmitterNode	0		
signal-Marble	Marble	-		
read-emitter	MarbleEmitterNode	0		
0-reader	MarbleEaterNode	+		
reader-Marble	Marble	+	0	0
1-reader	MarbleEaterNode	+		
eraser-emitter	MarbleEmitterNode	0		
garbage-collector	MarbleEaterNode	0		
eraser-Marble	Marble	+	1	1

Table 2: Summary of the particles in \mathcal{B} , with their most important attributes. Irrelevant values have been omitted: the bit can be made to work for multiple values of these variables. For the mass only the sign and not the magnitude has been recorded, except where the mass is 0. Note that it may not be strictly required to make those particles mass-less, but it simplifies the proof.

Let $\gamma \subseteq \mathbb{R}^3$ denote the smallest continuous cuboid region in \mathbb{R}^3 in which \mathcal{B} has influence (i.e. all particles of \mathcal{B} and all their attraction fields are contained in γ).

Lemma 4 (Reading state 0). *An external Marble can trigger architecture \mathcal{B} to increase the output of the 0-reader by 1 if the bit register is in the 0-state. After this operation, \mathcal{B} will be in the same state as it started except for the value of the 0-reader.*

Proof. Consider an external Marble that enters γ at the facet of γ that is closest to the reader-emitter, and let this Marble have velocity that moves it in a straight line to the reader-emitter. If this Marble has the correct mass, then the reader-emitter will emit a reader-Marble. This reader-Marble has an initial velocity in the direction of the 0-reader, by design of \mathcal{B} . Since there is no bit-Marble to alter its course of motion (since the bit is in state 0) nor any other attraction along its way, it will arrive at the 0-reader.

Note that the reader-Marble cannot intersect the radius of the bit-emitter, since the bit-emitter does not intersect the plane P , in which the reader-Marble remains its entire existence (it moves along the line from the reader-emitter to the 0-reader. These two Nodes are in P , and therefore this entire line is in P).

Clearly, no particles that existed before the external Marble entered γ have been changed during this operation, except for the state of the 0-reader. \square

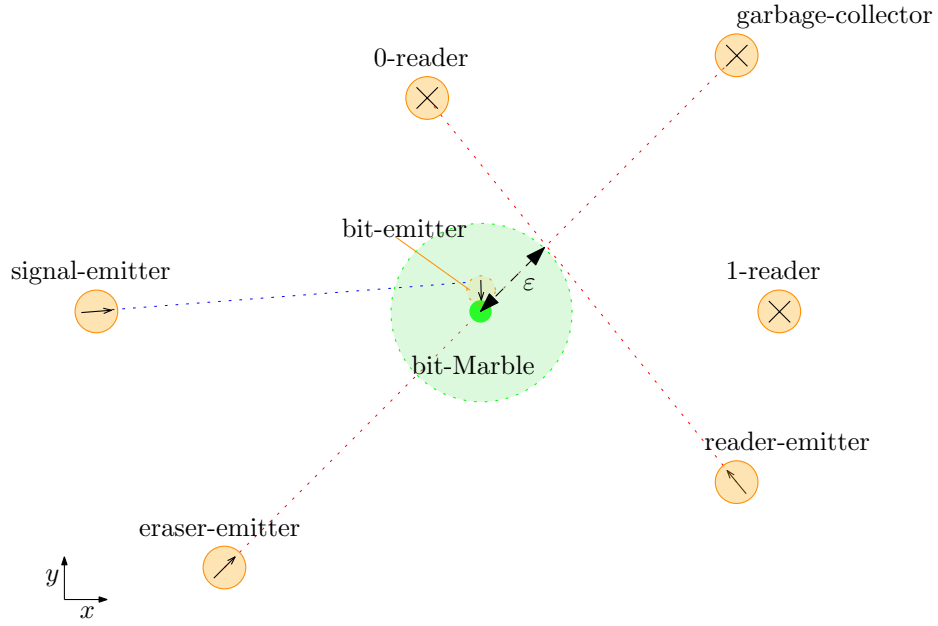


Figure 6: A visualization of the bit-register architecture \mathcal{B} , as projected on a 2-dimensional image. The Bit-Marble is drawn in green, with the threshold-gravity-radius drawn in light-green. Note that the distances and sizes are not necessary to scale. Hypothetical paths of emitted Marbles are sketched with dotted lines (hypothetical in the sense that the emitted Marbles would follow this path if no forces acted on it).

Lemma 5 (Reading state 1). *There exists a location for the 1-reader, a value for ε , a mass value and a gravity threshold value for the bit-Marble, such that an external Marble can trigger architecture \mathcal{B} to increase the output of the 1-reader by 1, if the bit register is in the 1-state. After this operation, \mathcal{B} will be in the same state as it started except for the value of the 1-reader.*

Proof. As in Lemma 4, an external Marble can cause the reader-emitter to emit a reader-Marble. Since the state of the bit is 1, there is a bit-Marble at the bit-position. Now we can adjust ε and the threshold of the bit-Marble's gravity such that the path of the reader-Marble will intersect the attraction field of the bit-Marble at its boundary. Let p the point where this boundary and the line between the reader-emitter and the 0-reader (which define ε) intersect.

The direction of movement the reader-Marble will not be altered from its starting velocity until it reaches point p . At this point, only the acceleration of the reader-Marble will be affected. This is true because the mass of the bit-Marble is, by construction, of the opposite sign as that of the reader-Marble, and because the reader-Marble does not attract Marbles while it is attracted by them (by construction). The reader-Marble will be accelerated in the same direction as the line segment between the bit-position and p , and this direction is orthogonal to the direction of the reader-Marble's initial velocity.

Since the reader-Marble intersects only shortly this acceleration is present only one instant of time. However, if the mass of the bit-Marble is of sufficient magnitude, it will change the direction of the velocity of the reader-Marble significantly. The new direction of this velocity is not the opposite of the original direction, as the acceleration was orthogonal to the original velocity of the reader-Marble. Hence the reader-Marble will not arrive at the reader-emitter (which requires the opposite direction as the original velocity of the reader-Marble had) nor the 0-reader (which requires the original direction).

Note that the reader-Marble cannot intersect the radius of the bit-emitter, since the bit-emitter does not intersect the plane P , in which the reader-Marble remains its entire existence. (As in Lemma 4, the entire path of the reader-Marble is in P . Since p is on the line between the reader-emitter and the 0-reader, p is in P as well. Now since the bit-position is also in P , the acceleration vector is also in P . The resulting velocity of the reader-Marble is a linear combination of its prior velocity and the acceleration, which are both vectors in P , hence the reader-Marble remains in P .)

The 1-reader can be positioned along the line from the reader-Marble in the new direction of the Marble's velocity, and then the reader-Marble will eventually be consumed by the 1-reader. \square

Lemma 6 (Writing bit). *An external Marble can trigger architecture \mathcal{B} when in state 0 (no bit-Marble present) to enter state 1 (with a bit-Marble present), without any other*

particle in \mathcal{B} being affected after completion.

Proof. Let the external Marble enter γ in the point closest point of the closest facet of γ to the signal-emitter, with a velocity the direction of the line from that point to the signal-emitter. Then this Marble will be consumed by the signal-emitter, and if it of sufficient mass it will trigger the signal-emitter once to emit a signal-Marble.

The signal-Marble is configured (by construction of \mathcal{B} to have a velocity in the direction of the signal-emitter towards the bit-emitter, and since it is not attracted by Marbles or Nodes, nor does any Eater- or EmitterNode block its path, it will eventually be consumed by the bit-emitter. Consequently, the bit-emitter creates a single bit-Marble. \square

Lemma 7 (Erasing bit). *An external Marble can trigger architecture \mathcal{B} when in state 1 (a bit-Marble present) to enter state 1 (no bit-Marble present), without any other particle in \mathcal{B} being affected after completion, except for the mass stored in the garbage-collector.*

Proof. Let the external Marble enter γ in the closest point of the closest facet to the eraser-emitter, with a velocity in the direction of the line from this point towards the eraser-emitter. The Marble will be consumed by the signal-emitter, and if the external Marble had enough mass, an eraser-Marble will be emitted in the direction of the bit position. Note that the eraser-Marble has both a Node- and Marble-stiffness of 1, hence no attraction force will affect its acceleration. Hence it will travel in a straight line with constant velocity.

The eraser-Marble has a Marble-stiffness of 1, and since the bit-Marble has a Marble-stiffness of 0, the bit-Marble's motion will be affected when the eraser-Marble nears the bit-Marble. Since the mass of the eraser-Marble is of the opposite sign as that of the bit-Marble, it will repel the bit-Marble, which will be accelerated in the same direction as the eraser-Marble is moving. Now we can adjust the masses of the bit-Marble and the eraser-Marble such that the repellent force is strong enough to accelerate the bit-Marble to the same or a higher velocity as the eraser-Marble before the eraser-Marble reaches the bit-position: this will guarantee that the eraser-Marble will not 'take-over' the bit-Marble and repel it in the other direction.

Now both Marbles will travel in the direction of the line from the eraser-emitter to the bit-position. By construction of \mathcal{B} , the garbage-collector is also on this line and on the other side of the bit-position as the eraser-emitter. Therefore both Marbles will eventually enter the radius of the garbage-collector and be absorbed. \square

We can summarize the results of Lemma 4, 5, 6 and 7 in the following theorem:

Theorem 8 (Bit register). *There exist settings for the parameters of \mathcal{B} , and an external Marble m outside of γ , such that by moving m with the right value of $m.vel$, $m.pos$ and $m.mass$ into γ :*

1. *m can trigger the reading of the bit. That is, after sufficient time, if there is a bit-Marble present, the 1-reader's number-of-Marbles-consumed count will increase by 1. If there no bit-Marble present, after sufficient time, the count of the 0-reader will increase by 1. When this count increases, the collection of particles in γ and their states are identical to the situation before m entered γ .*
2. *m can cause the creation of a bit-Marble in \mathcal{B} without affecting the state of other particles in \mathcal{B} .*
3. *m can cause the removal of a bit-Marble in \mathcal{B} , when present, without affecting the state of other particles in \mathcal{B} except for the Marbles consumed by the garbage-collector.*
4. *Furthermore, \mathcal{B} does not directly affect particles outside γ .*

Proof. 1. Follows from Lemma 4 and Lemma 5.

2. Follows from Lemma 6.

3. Follows from Lemma 7.

4. The particles in \mathcal{B} are constructed around a finite distance from the bit-position in \mathbb{R}^3 , use finite radii and are using the threshold gravity as attraction function with a finite threshold. Hence in each direction from the bit-position, there is a distance that surpasses the influence of attraction functions, radii and positions of particles. By construction of γ , the minimum value of this distance either defines a facet of γ or is interior to γ . Hence outside γ , \mathcal{B} cannot affect any particle directly.

□

3.4 Clock and divider

Implementing a clock in NENWIN is trivial: a MarbleEmitterNode with a large amount of `stored_mass` (e.g. a value of ∞) and a positively-valued delay will already periodically emit a Marble. Since Marbles are used to represent signals, this suffices to implement a periodical signal-creating device. However, the signal needs to reach multiple components after a sufficiently large delay, and a single Marble can be absorbed only once. Multiple clocks could be used, but a solution that reduces the amount of clocks needed is to use 'splitters':

Lemma 9. *Given a finite region $R \subset \mathbb{R}^x$ ($x \geq 2$) in a NENWIN architecture with no external forces, it is possible to construct an architecture in R such that when a Marble m with mass α enters R at a designated point q at t_0 , that this causes any fixed amount $n \geq 0$ Marbles to be emitted from R with velocities in different directions, at a time $t_0 < t_1 < \infty$. This architecture in R will not emit Marbles or exerts forces outside R otherwise.*

Proof. The case when $n = 0$ is trivial, a single MarbleEaterNode positioned in R with 0 Marble- and Node-attraction and a radius that intersects q .

For $n \geq 1$, consider the following architecture (where all particles have a Marble- and Node-stiffness of 1 unless denoted otherwise) (see also Fig. 7):

- Let P be a rectangle on a plane though R with maximal surface area.
- A 'signal-emitter': a MarbleEmitterNode, positioned such in P with such a radius that the border of the radius intersects the border of R . It has a delay of δ .
- Let l be the ray parallel to P that starts in the signal-emitter and that intersects the center of P .
- A 'signal-Marble': the Marble that can be emitted by the signal-emitter. Let it have a mass of α and a velocity direction parallel to the l (towards the centre of P) and a velocity magnitude of v_{signal} .
- Two 'locker-Nodes': two Nodes with the same negative mass, placed in P , both on a line l' in P orthogonal to l that also intersects the center of P , each at a different side of l , each at an equal distance from l . Their threshold distance of their attraction functions have the same positive value. Let these Nodes have a Marble-attraction of 0 and a Node-attraction of 1.
- A 'moving-emitter': a MarbleEmitterNode initially placed with a specific positive mass and a specific velocity v_{Node} at a specific point p' on l' where the distance to the closest locker-Node is $d + \varepsilon$, such that it will be deaccelerated by locker-Node untill it halts on a point p at a distance d from this locker-Node, and will reverse its direction when it is a distance d from that locker-Node: hence p' is an extreme point of the harmonic motion this moving-emitter will show. Let δ be the period of the harmonic motion. Let the moving-emitter have a delay of $\frac{\delta}{2 \cdot n}$. Let this Node be the only Node in R with a Marble- and Node-stiffness both of 0.
- Let v_{signal} equal $\frac{\varepsilon}{\frac{v_{Node}}{z}}$ where z is the smallest component parallel to l of the distance form the point where the signal-Marble is emitted to the border of the radius of the moving-emitter (which equals the distance from the point where the signal-Marble is created to the closest border of the signal-emitter when the latter

is in the point p).

- n 'output-emitters' named O_1, O_2, \dots, O_n , placed in P on the opposite side of l' as the signal-emitter is, such that at a time $t_0 + i \cdot \frac{\delta}{2 \cdot n} \bmod \delta$ the moving-emitter is in a position where a line-segment k_i exists in P that is parallel to l and intersects both the moving-emitter and O_i for $1 \leq i \leq n$, and such that the position and radius have that the border of their radius intersect the border of R .
- Let the 'split-Marbles' be the Marbles emitted by the moving-emitter with a mass of $\frac{\alpha}{2}$ and a velocity parallel to l (away from the center of P).

Note that the distance between each line segment k_i and k_j , $1 \leq i < j \leq n$ is not necessarily equal as the moving-emitter does not have a constant velocity and hence does not travel a fixed amount of distance in the same time span.

Now if m is consumed by the signal-emitter at time $t = t_0$, it will emit a signal-Marble. By construction of the moving-emitter, it will be at point p at time $t = t_1 = t_0 + \frac{\epsilon}{v_{Node}}$. But by construction, this is also the time required by the signal-Marble to travel to the point where it would be consumed by the moving-emitter if it were at point p . Since the moving-emitter is at point p , it will consume the Marble. By definition of point p , this is the point where the direction of the velocity of the moving emitter reverses in direction. So at time $t = t_1 + \frac{\delta}{2 \cdot n}$, by construction, the moving-emitter will be positioned on k_1 . Since its first delay has been satisfied, it will emit the first split-Marble, which is created in such a position where it will move in a direct line to O_1 . Now the `stored_mass` of the moving-emitter is $\alpha - \frac{\alpha}{n}$. The same process is repeated for O_2, O_3, \dots, O_n . Let \hat{p} the point that is the image of p when mirroring p in l on P . Because of the harmonic motion, the moving-emitter will reverse its direction again at point \hat{p} , but at this point its `stored_mass` is 0. Hence on the 'return trip' to p it will not emit any Marble. Now each of the output-emitters O_1, O_2, \dots, O_n has received exactly one split-Marble. Since each of the output-emitters intersects the boundary of R , each can create an output Marble outside R with a mass of $\frac{\alpha}{n}$, each in a different direction.

At time $t = \delta$, the moving-emitter is at point p' again with a `stored_mass` of 0, and if the velocity of the split-Marbles is large enough and the delay of the output-Marbles is small enough, all particles in R will be in the exact same state as at t_0 .

It remains to prove the harmonic motion of the moving-emitter. Note that if the threshold-distance of the locker-Nodes is at least as far as the distance to the other locker-Node, that the situation is equivalent to the physical model of simple harmonic motion under Newton's model of gravity [14]. It is beyond the scope of this report to prove simple harmonic motion, but the reader is referred to, for example, [19]. \square

Note that the NAND-gate requires both positively and negatively massed Marbles as 'power' from the clock to operate. This can be implemented by using two synchro-

nized MarbleEmitterNodes, one which emits positively massed Marbles, and the other negatively massed Marbles.

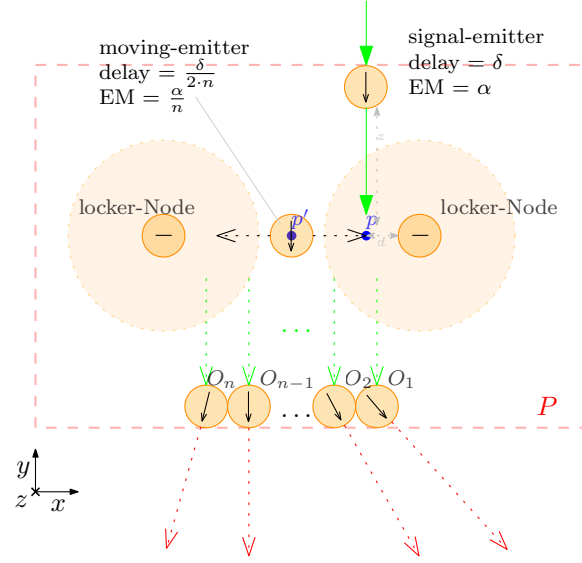


Figure 7: Construction as used in the proof of Lemma 9. The naming of objects is analogous with the proof. The black dotted arrows denote the directions of velocity of the moving-emitter, the red dotted arrows denote possible directions of velocity of the output Marbles, the green dotted arrows denote the last segment of the movement of the split-Marbles that are released by the moving-emitter, and the continuous green arrows denote the movement of the input-Marble and the signal-Marble.

3.5 Section conclusion

It is beyond the scope of this report to describe a complete implementation of a CPU in NENWIN, but sufficient important components have been described to abstract from the implementations of components, and reason on the (sequential) logical circuit level of abstraction. How to design a CPU with such circuits has been described in many sources, such as [4] and [16].

4 Training and backpropagation

As shown in the previous section, NENWIN is capable to simulate a CPU. Given that the RAM model is Turing complete, NENWIN is a Turing complete computational method as well. However, NENWIN has a very dynamic nature with complex interactions between particles, especially for larger architectures. This makes it unpractical to design architectures manually; automated optimization, or 'training', is needed for any practical application.

The goal of the training is to set up the architecture of Nodes, such that on a specific input $x \in \mathbb{R}^n$, $n \in \mathbb{N}^+$, given at a point in time $t = t_x$, leads to a desired output $y \in \mathbb{R}^m$, $m \in \mathbb{N}^+$ at a specific time $t = t_y > t_0$. Note that the way y is represented by the NENWIN model can be defined in multiple ways.

Only optimizing an given set of Nodes for classification will be explored in this section⁶. Classification tasks do not seem to exploit the dynamic nature of NENWIN, but are among the simplest task for initial experiments. This optimization will be done using the gradient-based backpropagation algorithm that is also commonly used to train neural networks. For mapping the gradients to an parameter update an off-the-shelf algorithm such as Gradient Descent or Adam [10] can be used. For this reason, only the derivation of the parameters gradients and the objective loss function will be described.

4.1 EaterNodes as output

For a classification task it is required that a model can output a prediction. This prediction can for example simply by a discrete class label, but also a probability distribution. In NENWIN it is straightforward to obtain a one-hot-encoding of discrete class label as output, by using MarbleEaterNodes. In this case, the output will simply be a vector of integers, where each value represents the number of Marbles eaten by each MarbleEaterNode. The MarbleEaterNodes may be ordered in any arbitrary fix order, as long as, at each point in time $t = t_j$, the output can be interpreted as an array with one value for each MarbleEaterNode.

This can be expressed more formally as defining a *cumulative output vector*:

Definition 1 (cumulative output vector). *Given a NENWIN model M , then for each point in time t , define the **cumulative output vector** $\vec{M}(t)$ as:*

$$\vec{M}(t)_i \equiv \text{number of Marbles eaten by the } i^{\text{th}} \text{ MarbleEmitterNode at time } t \quad (13)$$

⁶It is certainly not impossible to design optimization methods that also change the number of Nodes. For example, evolutionary algorithms may be suitable for this task. However, such methods are beyond the scope of this work.

Note that $\vec{M}(t)$ is always a vector of nonnegative integers, and at $t = 0$ we have $\vec{M}(0) = \vec{0}$.

4.2 Loss definition

The output of the model changes over time, and hence it is practical to define the 'real' output $\hat{\vec{y}}$ as the time-varying output read at a certain point in time. For convenience, call this time t_{end} . Then

$$\hat{\vec{y}} \equiv \vec{M}(t_{end}) \quad (14)$$

Given an expected output \vec{y} , the most straightforward way to define the *loss* of the 'real' output $\hat{\vec{y}}$ is to take a measure of difference between \vec{y} and $\hat{\vec{y}}$, such as the Mean Squared Error or the Cross Entropy Loss. However, this approach is not optimizable in all situations, as explained below.

4.2.1 Classification loss

Consider an application where a NENWIN model is used to classify an input as one out of k classes. Let each class-prediction be represented by a single MarbleEaterNode. Now since only one class is needed, the output $\hat{\vec{y}}$ can be read when the first Marble is eaten, or when the time $t = t_{max}$. More formally, let

$$t_{end} \leftarrow \min \left(\{t \mid 1 \leq |\vec{M}(t)|\} \cup \{t_{max}\} \right). \quad (15)$$

Now there are three possible cases for the output $\hat{\vec{y}}$ (for now, assume only one Marble will be eaten at $t = t_{end}$):

1. $\hat{\vec{y}} = \vec{y}$, and the loss can be set to 0.
2. $t_{end} = t_{max}$ and $\hat{\vec{y}} = \vec{0}$, that is, no Marble has been eaten.
3. $\hat{\vec{y}} \neq \vec{y}$ (and $\hat{\vec{y}} \neq \vec{0}$).

In case 2, it is expected that a Marble arrived at a specific MarbleEmitterNode n . However, there may be multiple Marbles present in the model, hence it is not clear *which* Marble should be eaten by n to achieve the desired output. The chosen method to resolve this is choosing the Marble m for which the loss would be smallest. Intuitively, this method 'blames' the Marble that seems most promising to be eaten by n for the loss. More formally, define:

$$L(\hat{\vec{y}}, \vec{y}) = \min_{m \in \text{Marbles}} f(m, n, t_{end}) \quad (16)$$

where

$$f(m, n, t) = \|n.pos(t) - (m.pos(t) + \mu \cdot m.vel(t))\|_2^2, \quad \mu \in \mathbb{R}_{\geq 0}. \quad (17)$$

Here μ is a nonnegative real number that functions as a hyperparameter.

The rationale behind including the ' $+\mu \cdot m.vel$ ' term is as follows: if only the position of the Marble is optimized, then it will be closer to n at $t = t_{end}$, but this does not necessarily imply it is also closer to being eaten by n . 'Almost being eaten' also requires m to be moving towards n ! ' $+\mu \cdot m.vel$ ' can be seen as a very naive prediction of the future position of m . The intent of this addition is to make it more likely that 'minimizing the loss function' correlates with 'making m being eaten by n '.

μ could be fixed as a hyperparameter, but this may cause undesired effects when the magnitude of $m.vel$ changes significantly. For example, if $|m.vel|$ and μ are both large, then $m.pos + \mu \cdot m.vel$ might be further from $n.pos$ than $m.pos$, even if the direction of $m.vel$ is from $m.pos$ towards $n.pos$ (i.e. the naive prediction *overshoots*). It may be wise to make μ a function of the magnitude of $m.vel$, e.g. to demand that $\mu \propto \frac{1}{|m.vel|}$.

For case 3, also (16) can be used for the missing Marble at the expected output MarbleEaterNode encoded in \vec{y} . However, there is also another Marble, m' , which was eaten by some node $n' \neq n$ (otherwise case 3 would equal case 2 or case 1), where n' is the MarbleEaterNode at the unique index i where $\hat{y}_i = 1$. Since m' is eaten at $t = t_{end}$, $f(m', n', t_{end})$ (using (17)) is well defined, and the following loss function would penalize m' moving towards n' :

$$L(\hat{\vec{y}}, \vec{y}) = -\frac{1}{f(m', n', t_{end})} + \min_{m \in Marbles} f(m, n, t_{end}) \quad (18)$$

The reciprocal $-\frac{1}{f(m', n', t_{end})}$ is used instead of $f(m', n', t_{end})$, as the latter will be small in magnitude (considering the Marble was eaten), but becomes larger the further m' is away from n' . But the further m' is away from n' , the less m' should be corrected.

It is possible to add scalar weights to each of the two terms $-\frac{1}{f(m', n', t_{end})}$ and $\min_{m \in marbles} f(m, n, t_{end})$, but this approach has not been explored further.

In summary, the loss $L(\hat{\vec{y}}, \vec{y})$ is defined as:

$$L(\hat{\vec{y}}, \vec{y}) = \begin{cases} 0 & \text{if } \hat{\vec{y}} = \vec{y} \\ -\frac{1}{f(m', n', t_{end})} + \min_{m \in Marbles} f(m, n, t_{end}) & \text{if } \vec{y} \neq \hat{\vec{y}} \neq \vec{0} \\ \min_{m \in Marbles} f(m, n, t_{end}) & \text{if } \hat{\vec{y}} = \vec{0} \end{cases} \quad (19)$$

Where n is the node at the unique index i where $y_i = 1$, $Marbles$ is the set of all Marbles in the model, and m' is the Marble eaten by some node $n' \neq n$ in the case $\vec{y} \neq \hat{\vec{y}} \neq \vec{0}$.

4.2.2 Multiple outputs

Eq. (19) assumes that at most one Marble will be eaten. It is possible that multiple Marbles will be eaten at the same time. Especially in simulation this is not unlikely, where discrete finite-sized time steps are taken.

Let k be the number of Marbles eaten at $t = t_{end}$, and let these Marbles be m_1, m_2, \dots, m_k . Let the corresponding MarbleEaterNodes that ate them be n_1, n_2, \dots, n_k . Note that these MarbleEaterNodes may not all be distinct, while the Marbles are all unique. Let n be the MarbleEaterNode of the correct (expected) output. Then we can extend (19) to:

$$L_{total}(\hat{\vec{y}}, \vec{y}) = \mathbb{1}(n \notin \{n_1, n_2, \dots, n_k\}) \cdot \min_{m \in \text{Marbles}} f(m, n, t_{end}) - \sum_{i=1}^k \frac{1}{f(m_i, n_i, t_{end})} \quad (20)$$

Where $\mathbb{1}(p)$ equals 1 if the proposition p is true, and 0 if p is false. In the very specific case that *all* Marbles have been eaten by the wrong Nodes, the term $\min_{m \in \text{Marbles}} f(m, n, t_{end})$ will not be defined. It was chosen to simply leave this term out in this case. If the penalty for the wrongly eaten Marbles causes sufficient change in the update rule, then (in the next iteration, or a few iterations later) there will be uneaten Marbles available to 'blame' for not being eaten by the correct MarbleEaterNode.

In other words:

- For each wrongly outputted Marble, the wrong-output penalty is added to the loss.
- In case the correct output was not included, also the missing-output penalty is added once.

Note that this method does not penalize multiple Marbles arriving at the correct output Node, which may in some contexts also be undesirable.

4.2.3 Non-convexity

Eq. (19) is not convex. This is not surprising given its relatively complex piece-wise definition.

The following lemma proofs that even optimizing the initial values (which are the initial position, velocity, acceleration and the mass) of particles, keeping the set of particles themselves constant, does not have a convex objective.

Lemma 10 (Non-convexity of (19)). *Assuming a constant vector \vec{y} , (19) is not convex, for all NENWIN architectures, in the initial values of the particles.*

Proof. For simplicity, we proceed with a specific counter-example. Consider an architecture with a single Marble m , two MarbleEmitterNodes E_1 and E_2 , and a MarbleEaterNode n . Let $\vec{y} = [1]$. Let both emitters have such a threshold and such a prototype that if they eat m , they will emit some new Marble m' that will move towards n and be eaten in $t' < \frac{1}{2}t_{end}$ time. Let $m.node_stiffness = 1$. Now position the four initial particles on the vertices of a sufficient large square that their radii do not overlap, and E_1 and E_2 oppose each other. Let A be the vertex assigned to m . The parameter of interest is now the initial velocity of m , in particular the *angle* of $m.vel(t_0)$. Let the magnitude of $m.vel$ be such that, under constant $\vec{0}$ acceleration and no obstacles, m would travel several times the length of an edge of the square. Now define the following angles $a_1 < a_2 < \dots < a_7$ of the direction of $m.vel$ (see Fig. 8):

- a_2 : $m.vel$ is directed towards E_1 , then E_1 would emit a Marble which arrives at n before $t = t_{end}$. Hence the loss would be 0.
- a_3 : $m.vel$ is directed towards the center of the edge of the square between E_1 and n . At $t = t_{end}$, m would still exist and be far from n , and hence the loss would be much greater than 0.
- a_4 : $m.vel$ is directed towards n and m will be eaten by n before $t = t_{end}$, the loss will be 0.
- a_5 : $m.vel$ is directed towards the center of the edge of the square between E_2 and n . The loss of this case is the same as in case 2 (i.e. nonzero).
- a_6 : $m.vel$ is directed towards E_2 . The loss of this case is 0, by symmetry with case 1.
- a_1 or a_7 : $m.vel$ is not directed to the inside of the square, nor parallel or close to parallel to one of the edges, nor to one of the regions within the radii of E_1 or E_2 . The loss will be nonzero as n will not eat any Marble.

\hat{y} is a function of the initial values of the particles and the angle of $m.vel$ is part of these initial values. The loss in the case of a_3 is larger than in the case of a_2 or a_4 (see also Fig. 9). Clearly this violates the convexity property, and hence (19) is not convex in the angle of $m.vel$, and hence not in all initial values of the particles. \square

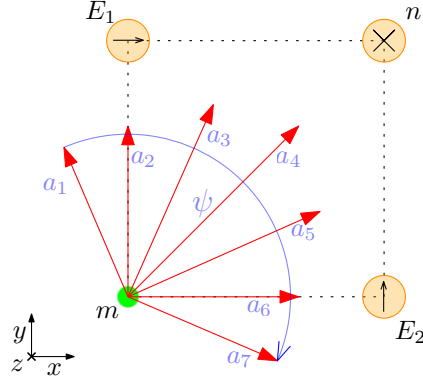


Figure 8: Sketch depicting the architecture used in the proof of Lemma 10. The red arrow depict the various angles ψ of the direction of $m.vel$.

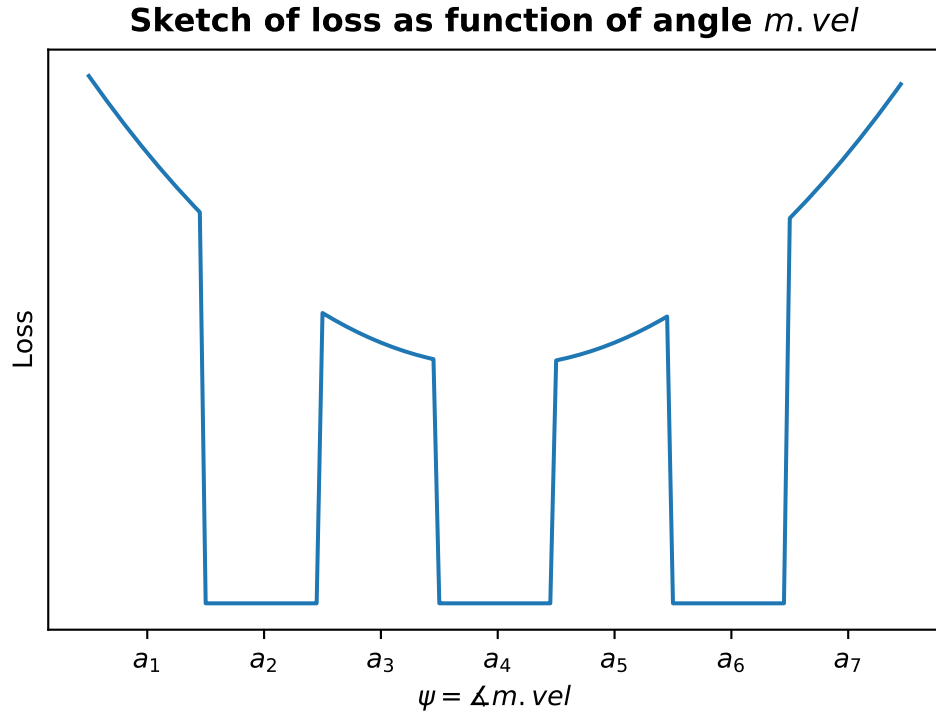


Figure 9: Sketch depicting loss function $L(\hat{\vec{y}}, \vec{y})$ as a function of the angle ψ of $m.vel$, in the architecture used in the proof of Lemma 10.

4.2.4 Loss gradient

Let p and s be particles, then define the *stiffness* function as:

$$stiffness(p, s) = \begin{cases} p.marble_stiffness & \text{if } s \text{ is a Marble} \\ p.node_stiffness & \text{if } s \text{ is a Node} \end{cases} \quad (21)$$

Using Eq. (4), (5), (6) and (7) to describe the state of some particle p at a point in time $t = t_1$, we can rewrite the state as follows (assuming that the amount of particles in the architecture is finite):

$$p.pos(t = t_1) = p.pos(t = t_1 - 0) + 0 = \lim_{\varepsilon \downarrow 0} \left(p.pos(t = t_1 - \varepsilon) + p.vel(t = t_1 - \varepsilon) \cdot \varepsilon \right) \quad (22)$$

$$p.vel(t = t_1) = p.vel(t = t_1 - 0) + 0 = \lim_{\varepsilon \downarrow 0} \left(p.vel(t = t_1 - \varepsilon) + p.acc(t = t_1 - \varepsilon) \cdot \varepsilon \right) \quad (23)$$

$$\begin{aligned} p.acc(t = t_1) &= \sum_{\substack{\text{particles } s \\ \text{acting on } p}} stiffness(p, s) \cdot \frac{p.mass \cdot s.mass}{p.pos(t = t_1 + 0) - s.pos(t = t_1 + 0)} \\ &= \lim_{\varepsilon \downarrow 0} \left(\sum_{\substack{\text{particles } s \\ \text{acting on } p}} stiffness(p, s) \cdot \frac{p.mass \cdot s.mass}{p.pos(t = t_1 - \varepsilon) - s.pos(t = t_1 - \varepsilon)} \right) \end{aligned} \quad (24)$$

Limits cannot be numerically represented on a digital computer. However, we can use a small finite-valued $\varepsilon > 0$, $\varepsilon \in \mathbb{R}$, and then it *approximately* holds that:

$$p.pos(t = t_1) = p.pos(t = t_1 - 0) + 0 \approx p.pos(t = t_1 - \varepsilon) + p.vel(t = t_1 - \varepsilon) \cdot \varepsilon \quad (25)$$

$$p.vel(t = t_1) = p.vel(t = t_1 - 0) + 0 \approx p.vel(t = t_1 - \varepsilon) + p.acc(t = t_1 - \varepsilon) \cdot \varepsilon \quad (26)$$

$$p.acc(t = t_1) \approx \sum_{\substack{\text{particles } s \\ \text{acting on } p}} stiffness(p, s) \cdot \frac{p.mass \cdot s.mass}{p.pos(t = t_1 - \varepsilon) - s.pos(t = t_1 - \varepsilon)} \quad (27)$$

Furthermore, note that for some $t_1 > t_0$, where t_0 is the starting time (at which each initially existing particle has its original position and velocity):

$$p.pos_0 = p.pos(t = 0) = p.pos(t = t_1 - t_1) \approx p.pos(t = t_1 - \varrho t_1) \quad (28)$$

for some positive constant $0 < \varrho < 1$ defined such that $\varrho t_1 \in \mathbb{Z}$.

We can use the above approximations to rewrite the position of a particle p as a recursive function though time depending on earlier states:

$$\begin{aligned}
p.pos(t = t_1) &= p.pos(t = t_1 - 0) + 0 \approx p.pos(t_1 - \varepsilon) + \varepsilon \cdot p.vel(t_1 - \varepsilon) \\
&\approx p.pos(t_1 - \varepsilon) + \varepsilon \left(p.vel(t_1 - 2\varepsilon) + \varepsilon \cdot p.acc(t_1 - 2\varepsilon) \right) \\
&\approx p.pos(t_1 - \varepsilon) + \varepsilon \left(p.vel(t_1 - 2\varepsilon) \right. \\
&\quad \left. + \varepsilon \cdot \sum_{\substack{\text{particles } s \\ \text{acting on } p}} stiffness(p, s) \cdot \frac{p.mass \cdot s.mass}{p.pos(t = t_1 - 3\varepsilon) - s.pos(t = t_1 - 3\varepsilon)} \right) \quad (29)
\end{aligned}$$

The terms $p.pos(t = t_1 - 2\varepsilon)$ and $p.vel(t = t_1 - 2\varepsilon)$ can again be expanded using (25) and (26). Assume that no MarbleEmitterNodes are present and no inputs are given. Consider the scenario where one continues this process, and applies (28) where this approximation is reasonable. If no circular recursion occurs (i.e. the sequence of substitutions does not produce a term that was previously substituted), then eventually an expression will be obtained in only the variables $k.mass$ and $k.pos_0$ for all particles k in the architecture. These variables are adjustable parameters, and the applied operations are division, multiplication and subtraction. Hence if the desired output time and location are known, then the Backpropagation algorithm can be applied, in combination with, for example, Gradient Decent, to optimize the architecture.

Now let m be an input that is given to the architecture at some time $t_{input} > t_0$. Let $m.pos_0 = m.pos(t_{input})$. Using Eq. (25), (26) and (27), which are all differentiable, we can recursively compute $\frac{\partial L}{\partial m.pos_0}$. Now recall that a NENWIN instance is defined with a function that maps external data to input Marbles (the `placement_funct` argument in the pseudocode Algorithm 1). If this function has learnable parameters, then $\frac{\partial L}{\partial m.pos_0}$ depends on those, and hence Backpropagation can optimize the function's parameters via $\frac{\partial L}{\partial m.pos_0}$.

4.3 Backpropagation of mass-gradient through MarbleEmitterNodes

Now consider a Marble m that is produced by a MarbleEmitterNode n . Let $n.spawnpos$ be the relative position of m with respect to n when m was emitted, and $m.pos_0$ be the absolute position where m was spawned. Now $m.spawnpos$ and $m.mass$ are parameters of n , and n is initially present in the architecture. A difficulty arises, since $m.pos_0$ depends on the time $t = \hat{t}_0$ at which m was created, which depends on the `stored_mass` of n . $n.stored_mass$ can be seen a non-smooth function of time and the set of consumed Marbles (which in turn depend on their initial position, attraction by other particles, their mass, etc.):

$$n.stored_mass(t) = \sum_{k \in n.eaten_marbles} k.mass - \sum_{h \in emitted_marbles(n)} h.mass \geq 0 \quad (30)$$

Where $emitted_marbles(n)$ denotes the set of Marbles previously emitted by n . This set only exist conceptually: no variable or attribute has been defined to track it.

One way to resolve this issue is to see the `stored_mass` together with the mass of the stored Marbles and the emitted mass as one continuum. In this case, $m.pos_0$ only depends on the last x consumed Marbles by n at $t = \hat{t}_0$ that together have sufficient mass, i.e.

$$x = \min_{\hat{x} \in \mathbb{Z}} \left(\hat{x} : \left(\sum_{i=\hat{x}}^{|n.eaten_marbles(\hat{t}_0)|} n.eaten_marbles(\hat{t}_0)[i].mass \right) \geq m.mass \right) \quad (31)$$

where we use the fact that `n.eaten_marbles` is a stack with references to the Marbles consumed by n . For convenience, call this set of x Marbles X .

Now between being consumed and being emitted, the quantity of mass that is $m.mass$ is 'frozen': it does not take part in any multiplication (except for the comparison whether m can already be emitted). Hence, under the assumption that $m.mass$ directly depends on the mass of the last x consumed Marbles (before m was emitted), and that inclusion in this set X directly depends on the *last* position of each Marble in X . It will be assumed that these direct dependencies can be modelled with a derivative of 1, i.e. for all $m_i \in X$ that are consumed by n at time t_i :

$$\frac{\partial m.pos_0}{\partial m_i.mass} = 1 \quad (32)$$

$$\frac{\partial m.pos_0}{\partial m_i.pos(t_i)} = 1 \quad (33)$$

Eq. (32) and (33) are the 'missing link' that allows Backpropagation through MarbleEmitterNodes. Note that strong assumptions have been made, that need to be justified by experimental results⁷. A disadvantage of this approach is that `n.radius` is considered to be fixed, and cannot be optimized.

4.4 Backpropagation of pos-, vel- and acc-gradient through MarbleEmitterNodes

The above description allows to find the gradient of the mass of an emitted Marble m with respect to the Marbles consumed by the MarbleEmitterNode n , and n itself. But also the gradient of the loss with respect to the initial position of the Marble can be used to optimize n . Note that m is created when certain variables (the time passed since last emit and $|n.stored_mass|$) exceed a certain threshold ($n.delay$ and $|m.mass|$).

$$m.pos_0 = n.pos(t) + n.spawnpos \quad (34)$$

$$\frac{\partial m.pos_0}{\partial n.pos(t)} = \vec{1} \quad (35)$$

$$\frac{\partial m.pos_0}{\partial n.spawnpos} = \vec{1} \quad (36)$$

⁷This will remain a topic for further research, as a better approach might be desirable.

4.5 Non-propagatable gradients

The position and the mass are special cases where the gradient of a loss with respect to a variable of the emitted Marble can be propagated back to the MarbleEmitterNode and the particles that influenced the MarbleEmitterNode. For other variables of the Marble, such as the initial velocity and acceleration, this does not seem to be the case. The acceleration is a function of the particles that are present in the neighbourhood of the place where the Marble is created, hence it is intuitive that this is not differentiable to the MarbleEmitterNode. For the velocity (and any other ordinary variable that extensions of Marbles may have) this might be less intuitive.

It can be shown by using a general case. Consider an object with variable v is created at a certain point in time $\hat{t} > 0$ where some time-varying variable $x(t)$ meets a certain threshold θ . Then initial value of v at \hat{t} , v_0 , can be written as a function of θ and x . Let \hat{v} be the predefined value that becomes *assigned* to v at $t = \hat{t}$. Note that *the value of* v_0 is independent of the value of $x(t)$ and vice-versa (v_0 is only created when $x(t) \geq \theta$, hence we always have $ReLU(\text{sgn}(|x(\hat{t}) - \theta|)) = 1$ when v_0 is created).

We have

$$v_0 = v_0(x(t), \theta) = \hat{v} \cdot ReLU(\text{sgn}(|x(\hat{t}) - \theta|)) \quad (37)$$

$$\frac{\partial v_0}{\partial x} = \hat{v} \cdot \frac{\partial ReLU}{\partial \text{sgn}} \cdot \frac{\partial \text{sgn}}{\partial x} \quad (38)$$

$$\frac{\partial v_0}{\partial \theta} = \hat{v} \cdot \frac{\partial ReLU}{\partial \text{sgn}} \cdot \frac{\partial \text{sgn}}{\partial \theta} \quad (39)$$

Add arguments to ReLU and sgn!

4.6 Backpropagation discussion

The training theory described above can only be applied if an output has been received. If no output is provided by the architecture, then it is ambiguous which Marble was required to be consumed by a specific MarbleEaterNode at a specific point in time. To resolve this, it is possible to assign a particular Marble a priori to be the output, or design the architecture in such a way that an output will always be given after sufficient time.

It is worth stressing that no known convex loss function exists for this optimization, so Gradient Descent might in general fail to find a global optimum. However, the attained local optima might still be of sufficient quality for the method to be of practical value. Further below, experimental performance will be discussed.

An alternative view on the reasoning above is that (25), (26) and (27) are a numerical integration of a system of differential equations. Following this line of thought, also other

explicit integration methods can be used for training. Since a numerical integration is needed in implementation to simulate the dynamics in Nenwin, this can effectively be combined with the training of the architecture.

5 Experimental results

The classification scheme as described above has been used on the Banknote Authentication dataset [7] (downloaded from [2]⁸). This particular dataset was chosen because it required only few particles to encode the input and the output:

1. There are only two distinct labels (binary classification).
2. Each input vector contains only four elements.

The implementation is available at <https://github.com/Nifrec/nenwin> under the open-source AGPL-3.0 licence[8]. The used programming language is Python [18], and the PyTorch framework [15] has been used to implement backpropagation.

Note that these experiments are intended to give an indication of trainability and parameter sensitivity of the NENWIN framework. A full search-space evaluation is beyond the scope of this report (and would require a more optimized implementation).

5.1 Dataset description

The classification task is to classify banknotes as genuine or as forgeries, given four derived features from the images. Class 0 has 762 samples and represent the genuine banknotes, class 1 has 610 represents the forgeries. This split is close to a 50%/50% split, meaning that random classification would yield an accuracy around 50%. The derived features (of Wavelet-transformed image) have been pre-computed, and are:

1. Variance
2. Skewness
3. Kurtosis
4. Entropy

For the experiments, the samples of the dataset were shuffled in a random order and split in a 80%/10%/10% train/validation/test set split. This split was cached and reused for each experiment (i.e. each experiment had the same train, validation and test set).

⁸Note that this page explains the labels the wrong way around. See [13]

5.2 Architectures

Three different architectures have been designed and were evaluated. See also Fig. 10.

In all architectures, all Nodes have their mass, `marble_stiffness`, `node_stiffness` and `marble_attraction` set to 1, and their `node_attraction` to 0. Note that these are only initial values for learnable parameters. The MarbleEaterNodes had their radius set to 0.5, which was not optimized by the implementation.

Architecture A:

- Vertices of input region: $(-2.5, -1)$, $(-2.5, 1)$, $(2.5, -1)$, $(2.5, 1)$.
- 4 non-output nodes surrounding the input region (positions $(0, -5)$, $(-5, 0)$, $(5, 0)$ and $(0, 5)$).
- MarbleEaterNodes (output Nodes) at $(-10, 0)$ and $(10, 0)$.

Architecture B: Same as Architecture A, but with additional Nodes at $(2.5, 2.5)$, $(-2.5, 2.5)$, $(2.5, -2.5)$, $(-2.5, -2.5)$.

Architecture C:

- Vertices of input region: $(0, 0)$, $(0, 1)$, $(6, 0)$, $(6, 1)$.
- 5 non-output nodes surrounding the input region (positions $(1, 2)$, $(2, 3)$, $(3, 2)$, $(4, 3)$ and $(5, 2)$).
- MarbleEaterNodes (output Nodes) at $(1, 4)$ and $(5, 4)$.

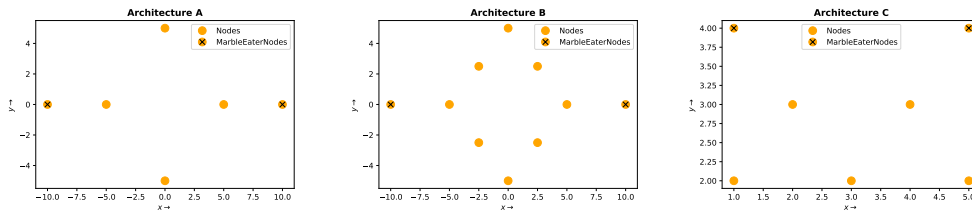


Figure 10: NENWIN Architectures used for training on the banknote dataset.

5.3 Setup

For each experiment, one of the architectures A, B or C was generated, and other hyperparameters were chosen. In particular, the batch size and the input placer were varied.

The training procedure used was as follows: during each epoch, the samples of the training set are iterated in a random order. Each sample in the training set converted to Marbles by the chosen input placer. Then the simulation is run until at least one MarbleEaterNode ate a Marble, or until a maximum number of steps is reached. Then the loss is computed according to (19), and gradients of parameters with respect to this loss are computed via backpropagation. Finally the parameters are updated using the Adam optimization technique [10].

The average gradients over the batch are used in case the batch size is larger than 1. The samples are still processed in sequential order, but the gradients of their losses are accumulated. The Adam update rule is only used after the last sample in the batch.

The value of μ in (17) was set to 1. Newton’s gravity function (without gravitation constant, (3)) was used as the attraction function for all particles. For all Marbles, both the `marble_stiffness` and `node_attraction` were set to 1, and both the `node_stiffness` and `marble_attraction` to 0.

Because of practical resource and time constraints, this maximum amount of timesteps was set to only 20 steps, with a stepsize of 0.1. With this configuration it took several hours to train an architecture⁹.

5.4 Results

Numerical results of various training-runs have been summarized in Table 3.

Most hyperparameter-configurations appear to provide poor results. A plot of the performance per epoch shows that the training initially makes progress, see Fig. 11. The loss decreases roughly exponential during the first epochs, and the validation accuracy roughly increases logarithmically. However, the training progress converges too quickly to mediocre performance.

One possible explanation for the poor performance of the VelInputPlacer, is that it gives the input Marbles a high initial velocity in varying directions. With a very limited amount of Nodes, the model may not possess the flexibility handle all combinations of initial velocity directions of the Marbles. The loss for the MassInputPlacer generally appears lower in Table 3. However, note that this only a hypothesis based on evidence,

⁹Training was run on a Intel(R) Core(TM) i7-7700HQ CPU @ 2.80GHz.

and not a statistically significant result.

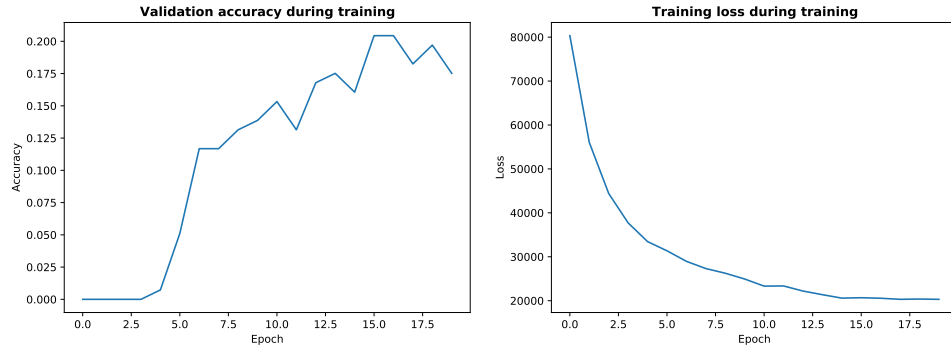


Figure 11: Performance of Architecture A as measured during each epoch of training. The `VelInputPlacer` was used to map the four banknote features to four Marbles. The batch size was 1. Note how the improvement of the accuracy on the validation set already seems to destabilize and cease rapid growth in less than 20 epochs. Given that the decrease in train set loss also flattened out at this time, it would seem unlikely that running more epochs would significantly increase the validation set accuracy.

Architecture	Timesteps	input placer	batch size	validation accuracy	training loss
A	20	VelInputPlacer	1	0.17518	20307.7
A	20	VelInputPlacer	2	0.13869	21173.4
A	20	VelInputPlacer	5	0.06569	28580.8
A	20	MassInputPlacer	1	0.0	13.5
A	40	MassInputPlacer($\begin{bmatrix} 0.5 \\ 0 \end{bmatrix}$)	1	0.29927	154.8
A	20	MassInputPlacer($\begin{bmatrix} 1 \\ 1 \end{bmatrix}$)	1	0.0	200.1
B	20	VelInputPlacer	2	0.12409	24788.9
C	20	VelInputPlacer	2	0.08029	33143.6
C	40	MassInputPlacer($\begin{bmatrix} 0.5 \\ 0 \end{bmatrix}$)	1	0.0	107.6
C	36	MassInputPlacer($\begin{bmatrix} 0.5 \\ 0 \end{bmatrix}$)	2	0.51825	-1198.1
C	40	MassInputPlacer($\begin{bmatrix} 0.5 \\ 0 \end{bmatrix}$)	2	0.20438	-4590.7

Table 3: Results of training a NENWIN architecture on the banknote-authentication dataset. Each row represents an independent training run. The accuracy is the total amount of correct predictions divided over the size of the validation set. Absence of output is counted as a wrong prediction. The loss accumulation of losses of the last epoch of the train set.

5.4.1 Evaluation eccentric run

The most surprising results are obtained with the MassInputPlacer with a velocity vector of $\begin{bmatrix} 0.5 \\ 0 \end{bmatrix}$, a batch size of 2, and using Architecture C as initial architecture. Note that Marbles will be moving towards the MarbleEaterNodes with this initial velocity in Architecture C. After 36 epochs this resulted in a validation-set accuracy above chance level, see Fig. 12. However, the learning curve shows very eccentric patterns. The high validation set accuracy after 36 epochs quickly disappeared after more epochs. This might be due to overfitting, although it is a very sudden change. The high non-convexity of the training objective may be a more likely explanation.

One hypothesis is that the optimization rule might have stepped a bit too far in a certain direction (by updating the parameters), and entered the domain of the loss function which has a different local minimum. This is for example possible if the optimization step caused a small adjustment that made a Marble being eaten early in the simulation, which would otherwise bypass the MarbleEaterNode. This would change the moment that the loss is computed. This may result in a very different loss, as the other Marbles will be at very different positions than at the end of the maximum simulation time. The Marble m' that was eaten may change the loss directly. If m' was eaten by a MarbleEaterNode n' (and n' represents the wrong prediction), then a new term $-\frac{1}{f(m', n', t_{end})}$ will be included to the loss. Since the distance of m' to n' will be very small, $f(m', n', t_{end})$ will be small, and the magnitude of the reciprocal term will be large.

The train-set loss also shows an extreme outlier, which occurs at the first epoch in the accuracy on the validation set experienced a sudden increase.

Also see Fig. 13 for a comparison of Architecture C before and after 40 epochs of training. The architecture has changed significantly. The output Nodes have been moved towards the input region. Also the mass of all Nodes has been decreased, among with some of the `attraction`- and `stiffness`-parameters (no Node had an increase). For example, the two MarbleEaterNodes had masses of 0.0753 and 0.0249¹⁰ (the starting values were both 1). But the normal Nodes had much higher masses: as high as 0.7981 (the lowest was 0.0981).

The same pattern was observed for the `marble_attraction`: it was much lower for the MarbleEaterNodes (0.0753 and 0.0015) than for the other Nodes (max: 0.7409, min: 0.0981, corresponding to the same 'normal' Nodes as the max and min mass). Apparently the model had learned that output Nodes should attract Marbles less strongly, as both the mass and the `marble_attraction` are used to compute the attraction force Marbles experience.

¹⁰Rounded to four figures. Also the other parameter values in this paragraph have been rounded to four figures.

The `marble_stiffness` remained close to 1 for most Nodes: only 1 'normal' Node had an extremely low value of 0.2775, and one MarbleEaterNode 0.5573 (for all others it was above 0.84). Apparently, the model did not learn to keep all Nodes stationary.

The test set score of this model, as obtained after 40 epochs, is 0.2174. The corresponding loss is -24058.3422 (both numbers are rounded to four figures). This is very close to the performance on the validation set.

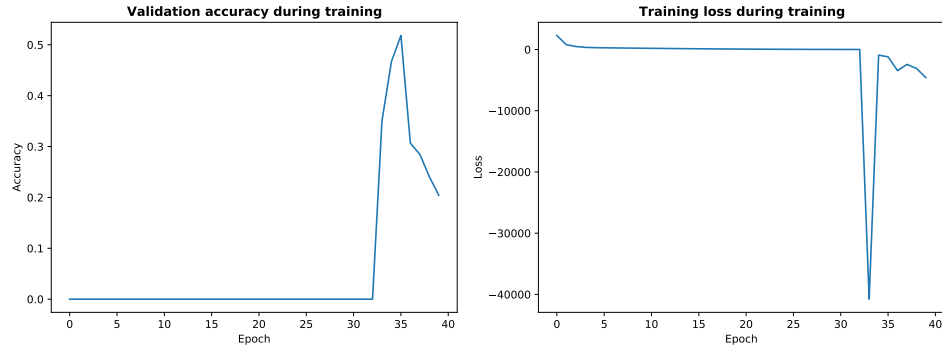


Figure 12: Learning curves of using Architecture C with a batch size of 2, $\text{MassInputPlacer}\left(\begin{bmatrix} 0.5 \\ 0 \end{bmatrix}\right)$ and 40 train-set epochs.

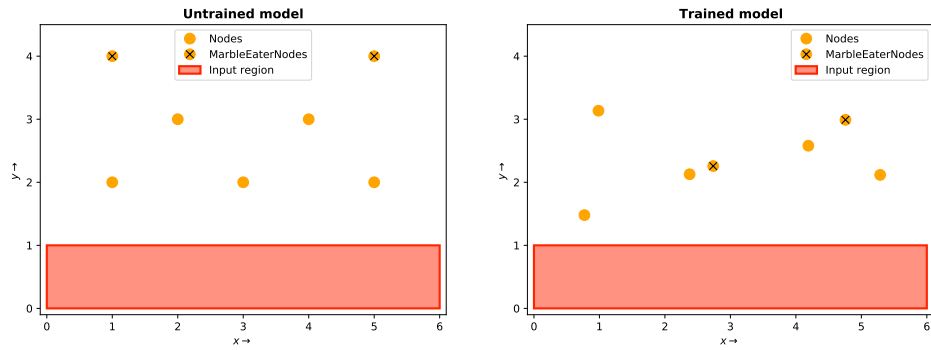


Figure 13: Architecture C before training (left) and after training on 40 epochs with a batch size of 2, $\text{MassInputPlacer}\left(\begin{bmatrix} 0.5 \\ 0 \end{bmatrix}\right)$.

5.4.2 A stable run with good performance

After the experiment described above, another configuration of hyperparameters was found that produced relatively good results (although still far below change level). This configuration uses Architecture A, a batch size of 1 and $\text{MassInputPlacer}\left(\begin{bmatrix} 0.5 \\ 0 \end{bmatrix}\right)$. The learning process is much more stable than the run above on Architecture C with the same input placer and batch size 2, but converges (with noise) before a high accuracy on the validation set is reached (see Fig. 14). It seems plausible that this is due to underfitting: with only four non-output Nodes, the model may have lacked adaptability. The test set accuracy of this model is only 0.0362 (rounded to four places).

Note in Table 3 that this configuration is very similar to the run with $\text{MassInputPlacer}\left(\begin{bmatrix} 1 \\ 1 \end{bmatrix}\right)$, while resulting in vastly different results on the validation set. However, from Fig. 14 it becomes clear that the first model did not change much in performance after 20 epochs, so this does not explain the difference in performance.

One hypothesis is that the nonzero horizontal component of the initial velocity biased the model using $\text{MassInputPlacer}\left(\begin{bmatrix} 1 \\ 1 \end{bmatrix}\right)$ towards one of the two outputs (in Architecture A, the MarbleEaterNodes are to the left and right of the input regions), but this does not sufficiently explain the validation set accuracy of 0%. The number of epochs were not identical, 40 and 20 respectively.

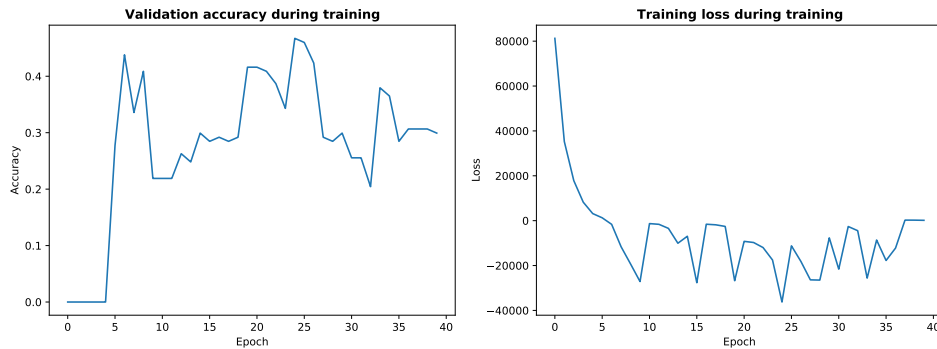


Figure 14: Learning curves of the run with Architecture A, a batch size of 1 and $\text{MassInputPlacer}\left(\begin{bmatrix} 0.5 \\ 0 \end{bmatrix}\right)$ trained on 40 epochs. Note that the curves are much more stable than in 12, although still noisy. It can also appear that the learning process converges to a steady noise after 5 to 10 epochs.

6 Complexity

This section will explore the runtime and memory complexity of the simulation of NENWIN. NENWIN itself is specified as a continuous system, mainly governed by Eq. (4)-(7). These differential equations cannot be analytically computed, so a discrete numerical integration approximation is used. With a specific integration algorithm in place, it is possible to derive the runtime complexity and the memory needs for backpropagation.

6.1 Beeman's Algorithm

Our implementation uses a variant of Beeman's Algorithm to numerically integrate Eq. (4)-(7). Beeman's Algorithm was first published by Schofield in 1972 [17]. The variant we used was published by Beeman himself in [3], and is a direct integration method. Applied to a particle p in NENWIN, we update the particle's motion each timestep as follows:

$$p.pos(t) = p.pos(t - h) + h \cdot p.vel(t - h) + \frac{1}{6}h^2 \cdot (4p.acc(t - h) - p.acc(t - 2h)) \quad (40)$$

$$p.vel(t) = p.vel(t - h) + \frac{1}{12}h \cdot (5p.acc(t) + 8p.acc(t - h) - p.acc(t - 2h)) \quad (41)$$

where h is the step-size and t the timestamp. Note that, at the beginning at timestep t , $p.acc(t)$ is computed according to Newton's gravity function (Eq. (3)).

6.2 Runtime complexity

Lemma 11 (Runtime complexity). *Assume a $\mathcal{O}(1)$ discrete numerical integration algorithm is used to compute a discrete approximation of (4)-(7) for a particle. Let m be a NENWIN architecture. Let T be the number of discrete timesteps the NENWIN algorithm is run on m . Let n be the number of particles in m . Then the number of operations needed to run the algorithm for t timesteps is bounded by $\mathcal{O}(T \cdot n^2)$.*

Proof. Refer to Algorithm 1.

Line 1 only copies a reference. Line 2 and 3 each do a constant amount of work for each Node, so are bounded by $\mathcal{O}(n)$. By definition of T , line 4 is executed T times. This is a loop with a long body, consisting of the following:

Line 13 iterates over all n particles. Line 14, within this loop, iterates over all other $n - 1$ particles. Line 15 is a $\mathcal{O}(1)$ operation. Hence the nested loops of lines 13-15 have an $\mathcal{O}(n^2)$ runtime.

The loops of line 16 and 19 iterate over a subset of all particles and all particles respectively, only only execute a constant amount of work within the loop body, and are hence both $\mathcal{O}(n)$. Finally the loop of lines 21-26 iterates over all Marbles and all MarbleEaterNodes, which are at most $\frac{1}{2}n \times 12n = \mathcal{O}(n^2)$ iterations.

So in total, the loop of line 4 makes $\mathcal{O}(T \cdot n^2)$ iterations, which is therefore also the upper bound of the algorithm. \square

6.3 Backpropagation memory complexity

Backpropagation requires a computational graph to be created during the simulation. This computational graph stores all algebraic operations applied and all constants needed to derive the partial derivatives of a loss with respect to all relevant the inputs and parameters of the simulation. This graph has a fixed size for a neural network, but in NENWIN it depends on the amount of simulated timesteps. To keep the theory brief, we will only consider NENWIN architectures without MarbleEaterNodes and MarbleEmitterNodes.

Lemma 12 (Backpropagation memory complexity). *Assume Beeman’s algorithm [17] is used to compute a discrete approximation of (4)-(7). Assume that Newtonian gravity (3) is used as attraction function. Let m be a NENWIN architecture. Let T be the number of discrete timesteps the NENWIN algorithm is run on m . Assume no MarbleEmitterNodes or MarbleEaterNodes are present in m . Let n be the number of particles in m . Let d be amount of dimensions used in m (i.e. the length of the pos, vel and acc vectors). Then the amount of memory needed to store all algebraic operations and numerical values in a computational graph for backpropagation is $\mathcal{O}(T \cdot n^2 \cdot (a_v \cdot d + a_s))$.*

Proof. Only the *pos*, *vel* and *acc* variables of a particle change in value. The *mass* (and optionally also the stiffness and attraction weights) do require gradients for optimization, but do not change value during simulation (only at the optimization step). Hence they are only leaves in the computational graph. By the same reasoning, the *initial* position, velocity and acceleration are leaves in the computational graph.

(3) uses one multiplication, a division, vector subtraction, a norm and a scalar square. No non-parameter constants are involved, so this requires an $\mathcal{O}(1)$ amount of memory to store the operations.

We proceed by considering the number of operations done on the *pos*, *vel* and *acc* of a single particle p in one discrete timestep (referring to Algorithm 1). Note that it requires only $\mathcal{O}(1)$ memory to store a *description* of a vector operation¹¹.

¹¹Only the references to the two operands, plus the operation itself, need to be stored. This is in contrast with the runtime of *performing* these operations, which depends on the size of the vectors. In case one of the operands is a constant vector literal it may need to be stored, but this is not the case in

1. Lines 13-14 compute the net force on a particle. Line 14 uses scalar subtraction and division (both take $\mathcal{O}(1)$ space), the norm of a length- d vector ($\mathcal{O}(1)$), and multiplication of a vector with a scalar ($\mathcal{O}(1)$ operations). The `attraction_function` is Newton's gravity function (bounded by $\mathcal{O}(1)$, as shown above). These operations are done for each of the other $n - 1$ particles (line 21), so a total of $\mathcal{O}(n)$ operations need to be stored.
2. Line 15 is a vector multiplication and an assignment, which take $\mathcal{O}(1)$ space to be stored.
3. Lines 19-20 execute Beeman's algorithm on each of the n particles. Beeman's algorithm require the previous acceleration, the previous position and the previous-previous acceleration to be cached, but these values are needed for backpropagation. This can be seen as follows, the partial derivatives of Eq. (40) are:

$$\frac{\partial p.pos(t)}{\partial p.pos(t-h)} = 1 \quad (42)$$

$$\frac{\partial p.pos(t)}{\partial p.vel(t-h)} = h \quad (43)$$

$$\frac{\partial p.pos(t)}{\partial p.acc(t-h)} = \frac{2}{3}h^2 \quad (44)$$

$$\frac{\partial p.pos(t)}{\partial p.acc(t-2h)} = -\frac{1}{6}h^2 \quad (45)$$

$$(46)$$

which are all scalars. The same reasoning holds for the partial derivatives of Eq. (41). Storing a fixed amount of scalars takes $\mathcal{O}(1)$ memory. Storing the operations itself also takes a $\mathcal{O}(1)$ amount of memory.

Hence, the total memory need for caching information for backpropagation for executing Beeman's algorithm on all particles is $\mathcal{O}(n)$ per timestep.

Since there are T timesteps, the total memory need is bounded by $\mathcal{O}(T \cdot n)$ □

The expression $\mathcal{O}(T \cdot n)$ may hide a large constant factor, and in practice it seems it indeed does so. Furthermore, for advanced applications many particles and many timesteps may be needed. Especially for numerical accuracy a large number of timesteps is desirable. Hence, despite the polynomial complexity, this can easily lead to a high memory cost.

Algorithm 1 (all vectors are variables).

7 Runtime complexity optimization

As shown above (Lemma 11), the runtime complexity of a single step of NENWIN is bounded by $\mathcal{O}(n^2)$. In practice, this complexity caused performance issues. However, there exist several approaches to improve the speed of the algorithm.

7.1 Limiting to neighbouring particles

By the nature of the gravity force function (Eq. (3)), a pair of particles at a large radius do not have significant interactions. For performance reasons, it is worthwhile to skip computing the forces these particles exert on each other (which sacrifices some accuracy). One approach to achieve this is to keep a list of pairs of particles that *do* interact, and only compute the interactions between these particles. If each particle is allowed to interact only with the nearest K particles, then the runtime complexity for a single timestep can be reduced to $\mathcal{O}(K \cdot n)$, which is significant if $K \ll n$. [1] and the introduction of [9] give an overview of applicable methods:

- **Verlet Neighbourhood list:** a maximum cutoff radius r_c and a neighbourhood-list radius $r_l > r_c$ are chosen. For each particle p a neighbourhood list is created. All particles within a distance of r_l from p 's location are considered neighbours and added to this list. During movement updates, all neighbours are iterated, and if they are within a distance r_c of p then the interactions between p and this neighbour is computed.

The speedup is achieved by recomputing the neighbourhood lists only after several timesteps, say k steps. The timesteps where the neighbourhood lists are not computed are faster, as only a strict subset (ideally small) of all possible particle pairs need to be compared. The distance $r_l - r_c$ works as a buffer, or a 'skin', to avoid the scenario where a particle enters the radius r_c of another particle p , without occurring on p 's neighbourhood list.

It was chosen not to use this method for NENWIN. It appears to be designed for predictable particles: for any of these predictable particles p , one can reasonably be sure that during k steps no particle that was at a greater distance than r_l from p (during the last neighbourhood-list computation) will come within a distance r_c of p . In NENWIN, the velocity of particles may vary quite heavily during a simulation, and the differences between the behaviour of architectures may be great. This makes it appear difficult to choose a safe value for k that still gives a sufficient speedup.

- **Cell-index method with large cells:** the space in which particles live is divided into a grid of 'cells'. The dimensions of a cell exceed the cut-off distance r_c . Thus, when

computing the interactions for a particle p in cell c , one only needs to consider the particles in c and the direct neighbouring cells of c . Assigning each particle to the correct cell is computationally cheap, and the limited set of potentially interacting neighbours for a particle p provides a major speedup.

- Cell-index method with very small cells: it is also possible to divide the space in which particles live into small cells in which at most one particle fits. Assigning particles to the correct cell is still cheap, and it can easily be computed which cells fall into a radius r_c (the cutoff-distance) of a given cell. This is not applicable to NENWIN, as Marbles and Nodes do not have a size (only MarbleEaterNodes and MarbleEmitterNodes have a `radius` attribute).
- Heinz and Hünenberger (2004): the algorithm proposed in [9] uses moderate-sized grid cells. It has three major steps: first, all particles are assigned to the grid cell they belong to. Then for each grid cell, the interacting cells are computing. Cells are interacting if the minimum distance between two particles of the different cells is below a threshold r_c . Finally, the interactions between particles are only considered for cells that were found to be interacting.

Note that all methods may still assign pairs particles with a larger distance than r_c to be neighbours, as they gather neighbours from a larger region than a sphere with radius r_c (for the first method the sphere has a radius $r_l > r_c$, and for the other method rectangular regions are used, at least in the 'vanilla' versions).

7.2 Application to Nenwin

It was chosen to create an algorithm inspired by the above to optimize NENWIN. It works as follows. The algorithm `PUTPARTICLESINBOXES` (Algorithm ?? below) creates a hyperrectangular grid over the space that contains all particles. In two dimensions this would be a regular grid of rectangles. The algorithm 'stretches' the grid such that it contains all particles. Then it simply creates a table, implemented as a tensor, mapping each grid cell to the containing particles.

The next step is to compute, for each box b_i , which other boxes are close enough for the particles to interact. It was not chosen to compute the minimum distance between any particle in b_i to any particle in the other box, as proposed in [9]. Instead, the minimum distance between (vertices of) boxes was used, regardless of the position of the particles within the box (this may be less accurate, but it is faster in the number of particles). This way, each neighbouring box of b_i is located in a roughly hypersphere-shaped space around b_i . The shape of this 'sphere' of neighbouring boxes is the same for each box, so it suffices to compute a mask of relative indices that can be transposed to the location of each box. After transposition, the mask gives the indices of the neighbouring boxes. `COMPUTEMASK` (Algorithm ??) generates such a transposable mask, given a

cut-off distance r_c . Note that some indices of the mask will need to be discarded after transposition, as they fall beyond the grid of boxes. The correctness of COMPUTEMASK is proven in Lemma 13.

Finally, it remains to integrate this procedure in the mainloop of NENWIN itself. `textscDistributedNenwin` (Algorithm ??) is a modified version of Algorithm 1. Each timestep, groups closeby particles in boxes using `PUTPARTICLESINBOXES`. Then it computes a neighbourhood mask, and for each box it computes the set of neighbouring boxes. A tuple of (1) the set of particles within a box and (2) the set of neighbours (including the particles themselves), is called a 'cluster'. Now the rest of the algorithm proceeds in a similar way as Algorithm 1, except that particle interactions are only computed between particles within a cluster (only the particles in the first set of the tuple are updated). This gives an opportunity for parallelism, as this can be done in parallel for the different clusters. Note that the processes need to synchronize between updating the movement and eating/emitting Marbles.

EATMARBLES, EMITMARBLES, UPDATEFORCES, UPDATEMOVEMENT are not described in depth, but correspond to the same operations in Algorithm 1. Only a few things are done differently:

- Each operates only on a subset of the particles, instead of all particles present in the model.
- UPDATEFORCES only updates the acceleration of the particles in its first argument, after computer the forces exerted on each of them by the particles in its second argument. Note that it is only ever called with the second argument being a superset of the first argument.

The following notation has been used in the pseudocode below:

- \odot for the element-wise product of two vectors.
- $indices(S)$ returns all tuples of valid indices for all tensors t with dimensionality S ¹².
- For any tensor T with D dimensions and an index $\vec{i} \in \mathbb{N}^D$, $T[*\vec{i}]$ is used to denote T indexed with the number in \vec{i} of the corresponding dimension, for each dimension. E.g. $T[*[1, 43]] \equiv T[1][4][3]$.

¹²Assuming S is of the form $S = S_1 \times S_2 \times \dots \times S_n$ where each $S_i \in \mathbb{N}$.

Algorithm 2:**PUTPARTICLESINBOXES** (**particles**, B)

Input: **particles** $\neq \emptyset$: A set of NENWIN particles. $B \in \mathbb{N} \setminus \{0\}$: number of boxes in any given dimension.**Output:** **boxes**: **boxes** a D -dimensional tensor (with B indices per dimension), of sets of particles that are in the same 'box'. \vec{l}_{tot} : vector with the lengths of the edges of the hyperrectangle that contains the boxes (and all particles).

```
1 Choose some arbitrary  $v \in \mathbf{particles}$  ;
2  $D \leftarrow \dim(v)$  ;
3 Let  $\vec{l}_{tot}$  be an empty array of length  $D$  ;
4 Let  $\vec{m}$  be an empty array of length  $D$  ;
5 Let  $\vec{l}_{box}$  be an empty array of length  $D$  ;
6 for  $d = 1$  to  $D$  do
7    $\vec{m}[d] \leftarrow \min\{p.pos[dim] | p \in \mathbf{particles}\}$  ;
8    $\vec{l}_{tot}[d] \leftarrow \max\{p.pos[dim] | p \in \mathbf{particles}\} - \vec{m}[d]$  ;
9    $\vec{l}_{box}[d] \leftarrow \frac{\vec{l}_{tot}[d]}{B}$  ;
10 Let boxes be a  $B^D$  tensor of empty sets.;
11 Define  $pos : \mathbb{N}^D \rightarrow \mathbb{R}^D$ , where  $pos(\vec{i}) = [\vec{l}_{box}[d] \odot \vec{i}[d] + \frac{1}{2}\vec{l}_{box}[d] \mid d \in \{1, \dots, D\}]$  ;
12 for  $p \in \mathbf{particles}$  do
13   if  $p.pos \neq p.prev\_pos$  then
14     Let  $index$  be an empty array of length  $D$  ;
15     for  $d = 1$  to  $D$  do
16        $index[d] \leftarrow \lceil \frac{p.pos[dim]}{\vec{l}_{box}[dim]} \rceil - 1$  ;
17     Add  $p$  to boxes[* $index$ ] ;
18 return boxes,  $\vec{l}_{tot}$  ;
```

Algorithm 3:**COMPUTEMASK(H, g, r_c)**

Input: H : a hyperrectangle $H \subseteq \mathbb{R}^D$ for some $D \in \mathbb{N} \setminus \{0\}$.
 g : a natural number $g \in \mathbb{N}$, the number of grid cell indices per dimension (when partitioning H into a regular grid of hyperrectangles).
 r_c : a cut-off radius $r_c \in \mathbb{R}_+$

Output: A set of relative indice-tuples $\vec{i} \in \{1, 2, \dots, g\}^D$ of grids cells such that for each present index, the corresponding hyperrectangular grid cell partially overlaps with a hypersphere placed at the center of H with radius r_c .

```
/* Compute sizes of grid cells */
1 Let  $\vec{s}_{cell} = \vec{0}_D$  ;
2 for  $d = 1$  to  $D$  do
3   Let  $H_d$  be the projection of  $H$  onto  $\vec{e}_d$ , where  $\vec{e}_d$  is the  $d^{th}$  column of the
   identity matrix  $I_d$  ;
4    $\vec{s}_{cell}[d] \leftarrow \min(H_d) - \max(H_d)$  ;
/* Compute set of all grid indices */
5  $indices \leftarrow \{-1, 1, 2, \dots, g\}^D$  ;
6  $M \leftarrow \emptyset$  ;
7 for  $\vec{i} \in indices$  do
/* Consider the lower-left vertex of each cell (generalized to
higher dimensions). */
8   if  $\|\vec{s}_{cell} \odot \vec{i} - \frac{1}{2}\vec{s}_{cell}\|_2 \leq r_c$  then
9      $M.add(\vec{i})$  ;
/* Also add the same cell mirrored around each possible
combination of axes. Note that  $(-1, -1)$  is the target
cell, and that some neighbours are added mutltiple times.
*/
10    for  $\vec{v} \in \{1, -1\}^D$  do
11       $M.add(\vec{v} \odot \vec{i})$  ;
12 return  $M$  ;
```

Note that, in implementation, M can be a tensor $T \in \{0, 1\}^D$ instead of a set. T has g indices for each of its D dimensions (i.e. T has the same shape as the grid in which H can be subdivided). For every grid position \vec{i} included in M , we would set $T[\vec{i}] = 1$, and 0 for the positions not present in M . This would make it faster to apply a mask using an optimized linear algebra library, but does not change runtime or memory complexity.

The following lemma proves the correctness of COMPUTEMASK. In particular, it shows that after translating the center of the 'mask' to a cell with indices \vec{j} , that the mask contains the neighbour cells of \vec{i} that are within a distance r_c .

Lemma 13. *Let $H \subseteq \mathbb{R}^D$ be a hyperrectangle. Let $G = \{\vec{j} : \vec{j} \in \{1, 2, \dots, g\}^D\}$ be a set of grid indices of the regular grid that subdivides H into smaller hyperrectangles, with g grid-cell indices per dimension. Let $0 < r_c \in \mathbb{R}$ be a positive radius. Let \vec{l}_H be a vector storing the length of H along each dimension. Then for all cell indices $\vec{j} \in G$, we have that $(\text{COMPUTEMASK}(H, g, r_c) + \vec{j} - 1) \cap G$ is the set of exactly all indices of all grid cells that have a minimum Euclidean distance of r_c or shorter to the cell indexed by \vec{j} .*

Proof. Assume any such H , D , G , g and r_c as described in the premise of the lemma. Take any arbitrary $\vec{j} \in G$. Let $R_i \subseteq H$ be the grid cell (a hyperrectangle) indexed by \vec{j} . Let $M = (\text{COMPUTEMASK}(H, g, r_c) + \vec{j} - 1) \cap G$. We now need to show that both:

- M does not contain the indices of any grid cell whose minimum Euclidean distance to a point in R_i is greater or than r_c .
- There does not exist a $\vec{p} \in G \setminus M$ such that \vec{p} indexes a grid cell at a minimum Euclidean distance of r_c or smaller to any point in R_i .

For contradiction, assume the negation of (1). So there exist a $\vec{p} \in G$ such that \vec{p} indexes a grid cell R_p such that the minimum Euclidean distance from any point in R_p to any point in R_i is larger than r_c . Let $\vec{p}' = \vec{p} - \vec{j} + 1$. Then we must have, by definition of M and \vec{p} , that $\vec{p}' \in \text{COMPUTEMASK}(H, g, r_c)$.

Refer to Algorithm ???. In line 7, all indices in *indices* are iterated. Note that *indices* = G . Let \vec{p}'' be the image of \vec{p}' mirrored in such a way around the axes that all its values are non-negative. Then one run of the loop will have $\vec{p}'' = \vec{i}$. Let R_p'' be the grid cell corresponding to R_p . Note that by the properties of translating \vec{p} to \vec{p}' and mirroring the latter to \vec{p}'' , R_p'' has the same minimum distance to the origin as R_p to the closest point in R_i . Hence this distance is greater than r_c . But then the comparison in line 8 fails, and no mirrored version (around 0, 1, ... or D axes) of \vec{p}'' will be added to M . As no other point in *indices* can be mirrored to become \vec{p}' , we can conclude that \vec{p}' was not returned by the algorithm and hence not in $\text{COMPUTEMASK}(H, g, r_c)$. This is a contradiction, hence the negation of (1) is false. Thus (1) holds.

Case (2) can be proven by the same reasoning, when one replaces 'greater than r_c ' by 'smaller or to r_c ' and removes 'not' from 'not in $M/\text{COMPUTEMASK}(H, g, r_c)$ '. \square

Algorithm 4:

DISTRIBUTEDNENWIN(*all_particles*, *attraction_function*, *P*, *T*, *B*, Δt , r_c)

Input: *all_particles*: A set of NENWIN particles.

attraction_function: A function: $\mathbb{R}^3 \rightarrow \mathbb{R}$ that maps the masses of two particles plus their distance to an attraction force.

$P \in \mathbb{N}_+$: number of parallel processes used.

$T \in \mathbb{N}_+$: number of simulated timesteps.

$B \in \mathbb{N}_+$: number of box-indices per dimension. Determines the total number of boxes used.

$\Delta t \in \mathbb{R}_+$: time passed between consecutive timesteps.

$r_c \in \mathbb{R}_+$: distance at which no interactions between a pair of particles are computed.

Output: None

```
1 for  $t = 1$  to  $T$  do
2    $grid, \vec{l}_{tot} \leftarrow \text{PUTPARTICLESINBOXES}(\text{all\_particles}, B)$  ;
3   Let  $H$  be the hyperrectangle, located at the origin, with edge lengths  $\vec{l}_{tot}$  ;
4    $M \leftarrow \text{COMPUTEMASK}(H, g, r_c)$  ;
5    $clusters \leftarrow \emptyset$ 
6   for  $\vec{i} \in \{1, 2, \dots, B\}^D$  do
7      $particles \leftarrow grid[*\vec{i}]$  ;
8      $neighbours \leftarrow \{grid[\vec{j}] : \vec{j} = \vec{m} + \vec{i} - 1, \vec{m} \in M\}$  ;
9      $neighbours \leftarrow neighbours \cap \text{all\_particles}$  ;
10    /* Note that  $particles$  is a subset of  $neighbours$ . */
11     $clusters.add((particles, neighbours))$  ;
12  Divide  $clusters$  into  $P$  disjoint subsets  $C = \{C_1, C_2, \dots, C_P\}$  ;
13  for ( $c \in C$ ) do in parallel
14    for ( $particles, neighbours$ )  $\in c$  do
15      UPDATEFORCES( $particles$ ) ;
16      UPDATEMOVEMENT( $particles, neighbours, \Delta t$ ) ;
17  for ( $c \in C$ ) do in parallel
18    for ( $particles, neighbours$ )  $\in c$  do
19      EATMARBLES( $particles$ ) ;
20      EMITMARBLES( $particles$ ) ;
21  /* The last operations may have added or removed particles. */
22   $\text{all\_particles} \leftarrow \{p : p \in \{c[1] : c \in C\}\}$  ;
```

8 Discussion

8.1 Extendability of Nenwin

The version of NENWIN present in this work can be seen as a specific subset of a more general computational scheme. This general scheme has a set of subclasses of particles (in the case of NENWIN there are two such subclasses, Marbles and Nodes), in which each particle has a `stiffness` and `attraction` parameter for each subclass in the architecture. Certain particles can 'eat' and/or 'emit' other particles of a specific class ¹³. One simple extension could be to introduce Nodes that can 'eat' and 'emit' other Nodes in a similar way to how `MarbleEaterNodes` and `MarbleEmitterNodes` eat and emit Marbles.

The specific subset of this generalized scheme is chosen as it was a small (but not proven to be *the smallest*) subset of particle-subclasses that was provably able to simulate a CPU.

8.2 Practical limitations

The empirical experiment in this work is of a very limited scope. It serves as an exploration of the trainability and hyperparameter-sensitivity of NENWIN, rather than a thorough scientific evaluation of the impact of specific hyperparameters on classification performance.

8.2.1 Unexplored hyperparameters

There are many hyperparameters that have been left unexplored. For example:

- Only three arbitrary architectures, all with a limited number of Nodes have been used. No `MarbleEmitterNodes` or architectures with a large number of Nodes have been investigated.
- The number of epochs were limited, it is worth investigating how the training process behaves over a longer time period.
- The maximum amount of timesteps per sample was very limited. Because a computational graph over all previous timesteps is needed to perform backpropagation, a larger number of timesteps would demand much more memory. It is possible the number of timesteps have a major impact on the loss function (as the position

¹³One may object to allowing a particle to 'eat' its own subclass, it that it would have to eat itself. However, it is possible to make an exception for themselves, or to add another workaround (e.g. hollow absorption regions instead of sphere-shaped).

of Marbles is different at another point in time). Hence also the outcome of the training may be very sensitive to the maximum amount of timesteps. This topic requires further investigation.

- Only one attraction function, one (rather large) timestep-size value and one value of μ in (17) were used.

8.2.2 Statistical significance

The comparison of different hyperparameter-configuration is potentially subject to heavy random noise. Because of the limited efficiency of the implementation, each experiment was only run once. The performance reached in training is a random variable, since each epoch over the train-set was iterated in a random order. As a result, no statistically robust conclusions can be drawn of the influence of specific hyperparameters on the performance of the model. It is left for future work to conduct many runs of each hyperparameter-configuration, and report the mean performance statistics (including confidence intervals).

8.3 Loss function

Two potential issues are observed from the empirical experiment:

- The loss function can become deeply negative. This is only to be expected based on Eq. 19. However, it seems unintuitive: a loss of 0 could indicate a correct prediction while a lower loss of -4000 can follow from a wrong prediction.
- The term that penalizes wrong predictions in the loss function (Eq. 19), namely $-\frac{1}{f(m',n',t_{end})}$, can suddenly subtract a large value from the loss function. Here 'suddenly' refers to a small adjustment from the previous parameter-update, that made a wrong prediction start to occur. This makes the loss function very noisy and sensitive, which may not be beneficial for the training progress.

8.4 A broader view

In a very broad sense, NENWIN is an experiment to use backpropagation and Adam (a variant of Gradient Descent) on a system that is not typically used for machine learning. In particular, the chosen system was a simplistic particle simulation. The question can be asked if other systems exist, such as scientific simulations of physics, chemistry, biology, etc., that are potential candidates as machine learning agents (which can be trained with backpropagation and Gradient Descent).

9 Conclusion

This work explored the possibility of using particle simulation as a trainable machine learning agent. A framework of particles, in particular Marbles and three types of Nodes, has been specified. It was informally shown that this framework is Turing-Complete. Theory has been devised for applying backpropagation and Adam (a variant of Gradient Descent) on the system. This includes an optimizable, albeit highly nonconvex, loss function. This theory has been implemented and several experiments on a classification task have been conducted. Evidence was found that the training can gradually increase the performance of models with the backpropagation-based training algorithm. However, no good performing choice of hyperparameters have been found. The best reached accuracy on the test set was 0.2174, while chance level is approximately 0.5. Furthermore, proposals have been made for improving the time and memory performance of the simulation, but these could not be tested empirically within the scope of this work.

10 Acknowledgements

I would like to thank Sibylle Hess for her technical advice and feedback, and Daan de Geus for his practical advice on organizing a project.

References

- [1] Michael P. Allen and Dominic J. Tildesley.
Computer Simulation of Liquids: Second Edition.
Oxford Scholarship Online, 2017, pp. 193–200. ISBN: 9780198803195.
DOI: [10.1093/oso/9780198803195.001.0001](https://doi.org/10.1093/oso/9780198803195.001.0001).
- [2] *Bank Note Authentication Data Set*. Data Science Dojo. 2019.
URL: <https://code.datasciencedojo.com/datasciencedojo/datasets/tree/master/Banknote%20Authentication>.
- [3] D. Beeman.
“Some multistep methods for use in molecular dynamics calculations”.
In: *Journal of Computational Physics* 20.2 (1976), pp. 130–139. ISSN: 0021-9991.
DOI: [https://doi.org/10.1016/0021-9991\(76\)90059-0](https://doi.org/10.1016/0021-9991(76)90059-0). URL:
<https://www.sciencedirect.com/science/article/pii/0021999176900590>.
- [4] Ahmet Bindal. *Fundamentals of Computer Architecture and Design*.
Springer, Cham, 2019. ISBN: 978-3-030-00223-7.
DOI: <https://doi-org.dianus.lib.tue.nl/10.1007/978-3-030-00223-7>.

- [5] Kyunghyun Cho et al. “Learning Phrase Representations using RNN Encoder-Decoder for Statistical Machine Translation”.
In: *CoRR* abs/1406.1078 (2014). arXiv: 1406.1078.
URL: <http://arxiv.org/abs/1406.1078>.
- [6] Stephen A. Cook and Robert A. Reckhow.
“Time bounded random access machines”.
In: *Journal of Computer and System Sciences* 7.4 (1973), pp. 354–375.
ISSN: 0022-0000. DOI: [https://doi.org/10.1016/S0022-0000\(73\)80029-7](https://doi.org/10.1016/S0022-0000(73)80029-7).
URL:
<http://www.sciencedirect.com/science/article/pii/S0022000073800297>.
- [7] Eugen Gillich and Volker Lohweg. *Banknote Authentication*. Nov. 2010.
- [8] *GNU Affero General Public License*. Version 3. Free Software Foundation.
Nov. 2007. URL: <https://www.gnu.org/licenses/agpl-3.0.en.html>.
- [9] Tim N. Heinz and Philippe H. Hünenberger. “A fast pairlist-construction algorithm for molecular simulations under periodic boundary conditions”.
In: *Journal of Computational Chemistry* 25.12 (2004), pp. 1474–1486.
DOI: <https://doi.org/10.1002/jcc.20071>.
eprint: <https://onlinelibrary.wiley.com/doi/pdf/10.1002/jcc.20071>.
URL: <https://onlinelibrary.wiley.com/doi/abs/10.1002/jcc.20071>.
- [10] Diederik P. Kingma and Jimmy Ba.
Adam: A Method for Stochastic Optimization. 2017. arXiv: 1412.6980 [cs.LG].
- [11] Alex Krizhevsky, Ilya Sutskever, and Geoffrey E. Hinton.
“ImageNet Classification with Deep Convolutional Neural Networks”.
In: *Commun. ACM* 60.6 (May 2017), pp. 84–90. ISSN: 0001-0782.
DOI: 10.1145/3065386.
URL: <https://doi-org.dianus.lib.tue.nl/10.1145/3065386>.
- [12] M.W. Matlin and T.A. Farmer. *Cognition, 9th Edition*. Wiley, 2016.
ISBN: 9781119177753.
URL: <https://books.google.nl/books?id=-r52CwAAQBAJ>.
- [13] James D. McCaffrey.
In the Banknote Authentication Dataset, Class 0 is Genuine / Authentic.
Aug. 2020. URL: <https://jamesmccaffrey.wordpress.com/2020/08/18/in-the-banknote-authentication-dataset-class-0-is-genuine-authentic/>.
- [14] Isaac Newton. *Philosophiæ Naturalis Principia Mathematica*. 1687.
- [15] Adam Paszke et al.
“PyTorch: An Imperative Style, High-Performance Deep Learning Library”.
In: *Advances in Neural Information Processing Systems* 32.
Ed. by H. Wallach et al. Curran Associates, Inc., 2019, pp. 8024–8035.
URL: <http://papers.neurips.cc/paper/9015-pytorch-an-imperative-style-high-performance-deep-learning-library.pdf>.

- [16] David Patterson and John Hennessy.
Computer organization and design - the hardware / software interface (3. ed.).
Jan. 2007. ISBN: 978-0-12-370606-5.
- [17] P. Schofield. “Computer simulation studies of the liquid state”.
In: *Computer Physics Communications* 5.1 (1973), pp. 17–23. ISSN: 0010-4655.
DOI: [https://doi.org/10.1016/0010-4655\(73\)90004-0](https://doi.org/10.1016/0010-4655(73)90004-0). URL:
<https://www.sciencedirect.com/science/article/pii/0010465573900040>.
- [18] *www.python.org*. Python Software Foundation. 2021.
URL: <https://www.python.org/>.
- [19] Hugh D. Young and Roger A. Freedman.
University Physics with Modern Physics, Global Edition. 14th ed.
Pearson (Intl), 2016. ISBN: 9781292100326, 129210032X.